DOI:10.14753/SE.2025.3062

SEMMELWEIS EGYETEM

DOKTORI ISKOLA

Ph.D. értekezések

3062.

MÉSZÁROS CINTIA

Alapkutatások klinikai alkalmazása
című program

Programvezető: Dr. Vásárhelyi Barna, egyetemi tanár

Témavezetők: Dr. Bárány László, PhD

Dr. Alpár Alán, egyetemi tanár

DOI:10.14753/SE.2025.3062

CLINICAL NEUROANATOMY OF THE SUBTHALAMIC AND SEPTAL REGION CONSIDERING THEIR ROLE IN DEEP BRAIN STIMULATION

PhD thesis

Cintia Mészáros

Semmelweis University Doctoral School

Theoretical and Translational Medicine Division

Supervisors: László Bárány, MD, Ph.D.
Alán Alpár, MD, D.Sc.

Official reviewers: Lajos Rudolf Kozák, MD, Ph.D.
Balázs Gaszner, MD, Ph.D.

Head of the Complex Examination Committee: Zsuzsanna Arányi, MD, D.Sc.

Members of the Complex Examination Committee: Tibor Kovács, MD, Ph.D.
Anita Kamondi, MD, Ph.D.

Budapest

2024

DOI:10.14753/SE.2025.3062

Table of contents

DOI:10.14753/SE.2025.3062

DOI:10.14753/SE.2025.3062

List of Abbreviations

ALIC:	anterior limb of the internal capsule
BNST:	bed nucleus of stria terminalis
CE:	Conformité Européenne
DBS:	deep brain stimulation
dMRI:	diffusion-weighted magnetic resonance imaging
DTI:	diffusion tensor imaging
FA:	fractional anisotropy
FDA:	Food and Drug Administration
FOD:	fiber orientation distribution
GPe:	globus pallidus externus
HCP:	Human Connectome Project
imMFB:	infero-medial branch of the medial forebrain bundle
MFB:	medial forebrain bundle
MSMT-CSD:	multi-shell multi-tissue constrained spherical deconvolution
MTT:	mamillothalamic tract
OCD:	obsessive-compulsive disorder
PFC:	prefrontal cortex
ROI:	region of interest
SCP:	superior cerebellar peduncle
slMFB:	supero-medial branch of the medial forebrain bundle
SMTh:	stria medullaris of thalamus
STN:	subthalamic nucleus
TRD:	therapy-resistant major depression
VTA:	ventral tegmental area

DOI:10.14753/SE.2025.3062

1. Introduction

Deep brain stimulation (DBS) is a functional neurosurgical procedure used in otherwise therapy-resistant neurological or psychiatric conditions. By DBS, electrodes are implanted in specific brain regions through which the functioning of this area can be modulated with electrical impulses which are controlled by a pacemaker-like device implanted usually under the clavicula. The main advantage of DBS over the destructive methods such as ablation or resection is its reversibility, so the treatment can be stopped at any time in case of unwanted side effects as well as by ineffectiveness. DBS was first used to treat psychiatric conditions and to relieve pain. The first permanent therapeutic electrode implantation took place in 1948 and is attributed to Lawrence Pool, who stimulated the head of the caudate nucleus of a patient suffering from depression and anorexia nervosa for several weeks, which improved the patient's condition. The era of modern DBS began in the 1980s, when stimulation has been introduced to relieve essential and parkinsonian tremor. To date, DBS is approved by the Food and Drug Administration (FDA) and Conformité Européenne (CE) with the following indications and targets: essential tremor, subthalamic nucleus (STN) DBS in Parkinson's disease, globus pallidus stimulation in Parkinson's disease, dystonia and severe obsessive-compulsive disorder (OCD). In 2010, DBS in intractable epilepsy also received CE-approval. In addition to the aforementioned indications, clinical trials and animal studies are ongoing in many other pathologies such as therapy-resistant chronic pain, Alzheimer's disease and various severe psychiatric conditions. [1–3]

Accurate anatomical knowledge of the targeted regions is essential for the safe and effective implantation of DBS electrodes. The aim of this thesis was to investigate and describe the topographical neuroanatomy of two brain areas significant for current or future DBS therapies: the subthalamus and the septum verum of the human brain. [**Figure 1**]

1.1.The human subthalamus

The human subthalamus is a complex region in the diencephalic-mesencephalic junction playing a role among others in movement regulation. The currently accepted description of this area is based on Forel’s observations supplemented later by Dejerine.

[4, 5] Forel distinguished 3 layers composing this area. According to his original depiction, the most ventral layer is formed by the STN, the intermediate by the zona incerta, which continues laterally in the reticular nucleus of the thalamus, and the dorsal layer („dorsal medulla of the subthalamus") which is very rich in myelinated fibers and since he regarded it the direct continuation of the mesencephalic tegmentum, he named it the H-field. (in German "Haubenfeld", hence the "H"). The H-field is divided into two parts lateral to the mamillothalamic tract (MTT): into a less defined, dorsal layer, which is continuous with the most ventral fiber bundles of the thalamus (Field H1) and a more ventral, flat layer (Field H2) which spreads out dorsal and rostral to the STN and its fibers pierce almost perpendicularly the internal capsule dividing it into smaller fiber groups. The H2-field is continuous with the fibers corresponding to the ansa lenticularis at the medial edge of the internal capsule and rostrally with the substantia innominata. [4]

According to the classical literature, the fibers passing through the subthalamic region consist mainly of pallidofugal fibers, which terminate in the thalamus (pallidothalamic fibers), in the STN (pallidosubthalamic fibers) and in the tegmentum of the mesencephalon (pallidotegmental fibers). Most of the pallidothalamic fibers run along the lenticular fasciculus (corresponding to Forel's field H2) and the ansa lenticularis, which merge in the prerubral area (corresponding to Forel's field H) from where they pass dorsolaterally to form - along with fibers from the superior cerebellar peduncle (SCP) and sensory afferents of the lemniscal system - the thalamic fasciculus (corresponding to Forel's field H1) and terminate in different parts of the thalamus. The ansa lenticularis runs on the basal surface of the pallidum, then curves around the cerebral peduncle to reach the subthalamic region. The fibers of the lenticular fasciculus, on the other hand, traverse the internal capsule, along with the pallidosubthalamic (and subthalamopallidal) fibers (i.e. the subthalamic fasciculus). [4–7]

The subthalamus and its connections include several DBS targets, primarily with the indication of movement-, but also various psychiatric disorders. [8, 9] The STN is one of the most targeted structure, the stimulation of which has been approved by the FDA for the treatment of tremor mainly in Parkinson's disease. [2] Since this nucleus is surrounded by numerous fiber bundles which could also be activated during stimulation, it is often not clearly understood exactly which fiber connections are responsible for the therapeutic or side effects. An important group of postoperative issues are

neuropsychiatric disturbances such as hypomania. [10] Based on their results obtained with deterministic diffusion tensor imaging (DTI) tractography, Coenen et al. suggested in their study that the background of this side effect may be the co-activation of the medial forebrain bundle (MFB) that courses in the close vicinity to the medial part of the STN. [11]

1.2.The medial forebrain bundle

The MFB is a group of fibers that connect the autonomic and limbic structures of the forebrain with the hypothalamus and the brainstem. [7] This fiber tract is well-described in rodents for a long time, but the first description of its course in the human brain was published hardly more than a decade ago using deterministic DTI tractography. [11, 12]

1.2.1. Classical definition of the medial forebrain bundle

According to the classical description, the MFB is a central pathway of the limbic system, which consists of loosely arranged, particularly thin fibers running in a rostrocaudal direction through the lateral hypothalamus between the basal forebrain areas and the midbrain tegmentum and considered to be a part of the reward system. The fibers of the MFB connect the monoaminergic cell groups of the brainstem with the lateral hypothalamus, bed nucleus of stria terminalis (BNST), amygdala, the nucleus accumbens and several other brain areas, but it forms a discrete fiber bundle only in a few places. It is a well-developed connection in non-mammalian vertebrates but relatively small in humans. [6, 7] Although there are some schematic depictions about the course of the human MFB in the classical literature, it is important to emphasize that these are based on results originally inferred from animal studies. To date, no study in the literature has directly showed the course of the MFB in the human brain.

1.2.2. Anatomical description of the medial forebrain bundle in humans

Coenen et al. presented the first description of the human MFB with deterministic DTI-tractography. [11, 12] According to their findings, the human MFB is different from that described originally in rodents and consists of two branches. The infero-medial

branch (imMFB), which is equivalent to the rodent MFB, runs in a longitudinal direction along the lateral wall of the third ventricle and terminates in the lateral hypothalamus. A second, supero-lateral branch (slMFB) leaves the former fiber stream in the region of the ventral tegmental area (VTA) and runs more laterally, undercrosses the thalamus (hence courses through the subthalamic region) and then passes through the ventro-lateral part of the anterior limb of the internal capsule (ALIC) to reach the nucleus accumbens and the prefrontal cortex (PFC). [11, 12] Prior to the publication of Coenen et al., no description mentioned that the MFB would pass through the ALIC. However, since then, several diffusion-weighted magnetic resonance imaging (dMRI) fiber tracking studies have been published with similar results. [13–20]

In the recent years, the definition of the human MFB has also been extended based on further investigations by tractography ("greater MFB system") and characterized as a prominent fiber pathway that connects the VTA to an extensive area of the cerebral cortex, such as motor cortical areas and the cerebellum ("motorMFB"), in addition to its limbic parts consisting of the slMFB and imMFB. [21, 22] However, no anatomical study yet validated these findings obtained purely with tractography.

1.2.3. Deep brain stimulation of the human medial forebrain bundle

After that Coenen et al. suggested that the background of hypomanic symptoms may be the co-stimulation of the MFB [11], this fiber bundle rapidly became a promising DBS target primarily in therapy-resistant major depression (TRD) [13, 23–25] but also in OCD. [26]

1.3. The human septum verum

The septum telencephali is a midline forebrain region between the cerebral hemispheres. The anatomy and connections of the septal area have been extensively discussed in various animal species, but investigations related to the septum in humans are rather lacking. For a long time, the human septum was considered as a vestigial structure, to which no particular importance or function was attributed. Andy and Stephan aimed first the detailed description of this area and showed in their comparative histological study that this brain region is actually well-developed also in humans. [27]

They distinguished two parts of the human septum: the dorsal located septum pellucidum and the more ventrally laying septum verum. The septum pellucidum is a phylogenetically new formation, it can only be found in higher primates and humans as its development occurs due to the rapid growth of the corpus callosum. The septum verum contains most of the septal nuclei and corresponds to the septum of the lower animals. [27] Later on, only Horvath and Palkovits investigated the structure of the human septum in depth and created a topographical atlas about this region based on histological serial sections. [28] They distinguished a medial area containing the medial septal nucleus, the triangular nucleus and the nucleus of the diagonal band as well as a lateral area consisting of the dorsal and lateral septal nuclei. [28]

Despite its relatively small size in the human brain, the septum is connected to many other areas, which reflects its role in complex operations. One of the most important connections of the septal region is the bidirectional septo-hippocampal pathway, which is carried out primarily via the precommissural fornix. However, the exact function of the septal region is still not fully understood. Our current knowledge is derived mainly from animal experiments and some early human studies which suggest that it is an essential part of the limbic system and has a key role in various behavioral and memory functions. [29–31] As a significant cholinergic center along with other basal forebrain nuclear groups, such as the nucleus basalis of Meynert and the diagonal band of Broca, the medial part of the septum forms an important organization with the hippocampus and plays a significant role in the generation of theta oscillations, the alteration or disturbance of which is a common observation in various pathological conditions. [32]

Animal experiments proved the positive therapeutic effects of stimulation of the medial septum by restoring or imitating the physiological hippocampal oscillation. Based on these promising results, the medial septum was proposed as a possible target of DBS with the indications of treatment-resistant temporal lobe epilepsy [33], cognitive impairment after traumatic brain injury [34], Alzheimer’s disease [32], various psychiatric disorders [32], and chronic pain. [32]

DOI:10.14753/SE.2025.3062

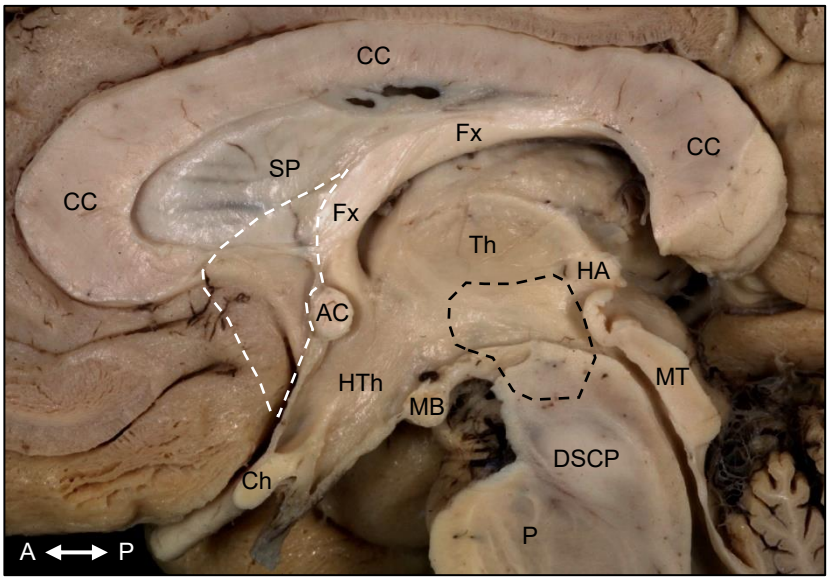

Figure 1 – The positions of the two regions discussed in this thesis on the medial surface of the brain

The white dashed line indicates the septum verum and the black dashed line the position of the subthalamic region. *Figure legend: AC: anterior commissure; CC: corpus callosum; Ch: chiasma opticum, DSCP: decussation of the superior cerebellar peduncle; Fx: fornix; HA: habenula; HTh: hypothalamus; MB: mamillary body; MT: mesencephalic tectum; P: pons; SP: septum pellucidum; Th: thalamus. Compass: A: anterior; P: posterior*

DOI:10.14753/SE.2025.3062

2. Objectives

The aims of this thesis were as follows:

Examination of the subthalamic region:

- Accurate description of the topographical anatomy of the human subthalamic region and its connections promoting the efficiency and safety of future DBS therapies.
- Investigation of the neuroanatomical causes of therapeutic or side effects occurring during DBS therapy of this region.
- Elucidation of the neuroanatomy of the human MFB as a structure topographically closely related to this area according to the literature.

Examination of the septal region (unpublished study):

- Accurate description of the topographic anatomy and connections of the human septum verum as a potential future DBS target.

DOI:10.14753/SE.2025.3062

3. Methods

The macroscopic and histologic studies in this thesis involved 24 formalin-fixed human brains. The cadavers were donated with educational and research purposes to the Department of Anatomy, Histology and Embryology of the Semmelweis University. The tractography studies involved 100 healthy subjects from the open-access Human Connectome Project (HCP) database. [35]

3.1. Fiber dissections

In the study of the subthalamic region 19, while for the investigation of the septal region 28 brain hemispheres were prepared and dissected according to the method of Klingler. [36] To facilitate the precise separation of the white matter fibers, a special in-situ fixation method was used to prevent the deformation of the brains and preserve the original anatomical position of the structures. After cannulation of the internal carotid and vertebral arteries on both sides, the blood vessels were flushed with 0.9 % saline and perfused with 4% formalin solution. The brains were carefully removed after a maximum of 72 hours post-mortem time, then immersed in 4% formalin solution as usual for at least 2 months. After the fixation process all brains were frozen in water at -30 °C for at least 2 weeks, then thawed out at room temperature and cut in the mid-sagittal plane. The dissections were performed in medial to lateral direction under 7x magnification of a stereomicroscope (Wild Heerbrugg, Switzerland) and with the aid of microsurgical instruments and self-made bamboo sticks. Photos were taken after each step of the dissections using 50- and 100-mm macro-objectives mounted on a Canon EOS 5D Mark I body (Canon Inc., Japan).

3.*2. Histology*

To validate our findings obtained with fiber dissections, one additional hemisphere was prepared for histological examinations. A tissue block containing the area between the anterior edge of the caudate nucleus and the decussation of the SCP was made. The lateral borders of the block were the cut surface of the brain in the mid-sagittal plane medially and the lateral part of the putamen laterally. The block was then manually cut into approximately 0.5 mm thick slices in the coronal plane. All slices of the block were

then fixed in 4% buffered formalin solution for an additional week. After the fixation, dehydration and clearing processes, the slices were embedded in paraffin. 8 μm thick serial sections were made from the whole brain-block with 32 μm spaces between the slices and stained with silver impregnation of the neurofibrils according to the method of Krutsay. [37] This staining method makes the cytoskeletal elements of the neurons visible, thus the cytoplasm of the nerve cells as well as the axons and dendrites became observable on the sections making it possible to trace the fiber bundles even if they are not myelinated. By the evaluation of some of the histological sections, circular polarized light was used to increase the contrast between the individual fiber bundles. With this method, fiber bundles with different orientations appear in a darker or lighter color compared to each other, which makes it easier to separate them.

During the fiber dissections of the septal region, 12 additional samples were removed randomly and stained with Luxol fast blue combined with Sirius red to validate the course of the dissected fibers.

3.3. Tractography

Beside the cadaveric investigations, the reconstruction of the human MFB was also aimed involving 100 healthy subjects (age between 26-35 years, 50 women, 50 men) of the HCP [35] using dMRI-tractography. Whole-brain tractographies were performed by means of the open-source MRtrix3 software package (version 3.0.3) [38] using two reconstruction algorithms: probabilistic DTI and Multi-Shell Multi-Tissue Constrained Spherical Deconvolution (MSMT-CSD). [38–41] A total of 1 million streamlines were reconstructed with both methods in all of the cases using grey matter/white matter interface seeding (based on co-registered T1-weighted images, see **Figure 2**) and 5 different cutoff values for both methods (0.2, 0.23, 0.25, 0.27 and 0.3 fractional anisotropy levels (FA) for DTI and 0.07, 0.1, 0.13, 0.15 and 0.17 fiber orientation distribution (FOD) thresholds for MSMT-CSD). All other parameters such as step size, angle threshold and minimal/maximal fiber length were left as default. [see 38–41]

DOI:10.14753/SE.2025.3062

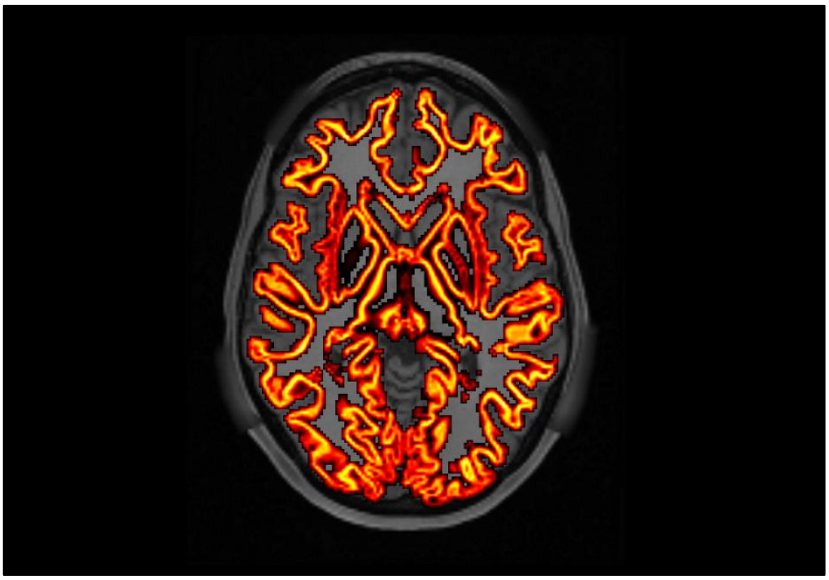

Figure 2 – Region of interest on an axial T1-weighted magnetic resonance (MR) image using grey matter/white matter interface seeding

Using co-registered structural T1-weighted MR-images, the automatically segmented border between grey and white matter was used as seed region (orange) to obtain whole-brain tractograms.

The slMFB was isolated from the whole-brain tractogram using a 5x5x5 mm^3 cubic region of interest (ROI) between the red nucleus and the MTT according to Coenen et al. [12] as well as a ROI in the ALIC placed in the coronal plane at the level of the anterior commissure. To determine the proportion of streamlines corresponding to the slMFB in the ALIC, also the streamlines passing through the ALIC were separately isolated using the same ROI as in the first step. All ROIs were manually defined to ensure their correct anatomical position in each cases. [**Figure 3**]

DOI:10.14753/SE.2025.3062

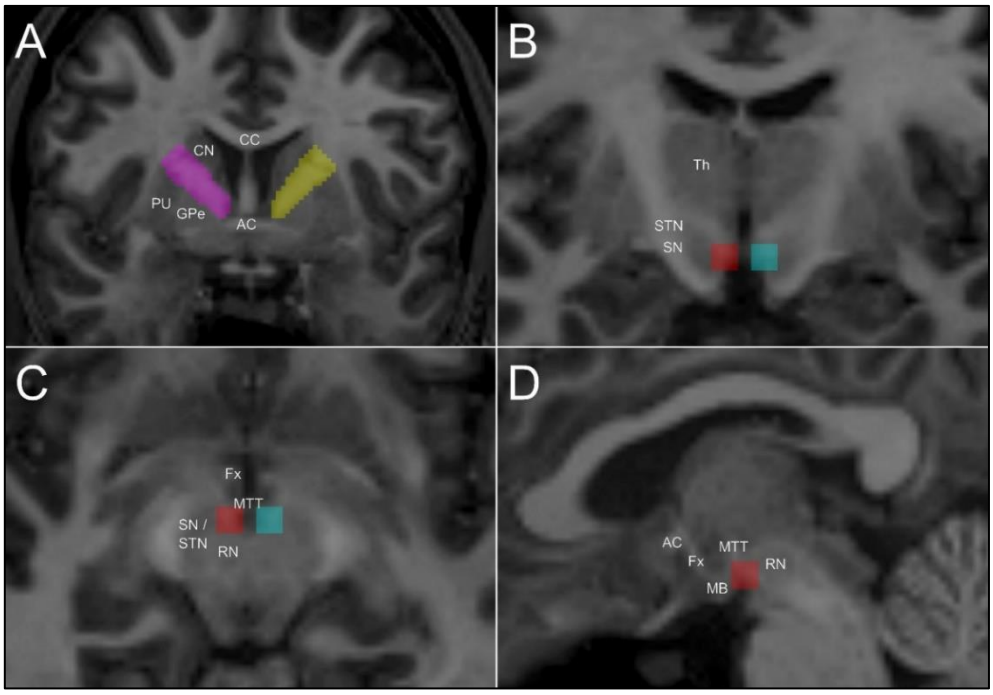

Figure 3 – Region of interests (ROI) used for track-selection of the superolateral branch of the medial forebrain bundle (slMFB) from the whole-brain tractogram [42]

Panel A: ROIs placed both sides in the anterior limb of the internal capsule in the coronal plane at the level of the anterior commissure. Panel B-D: ROIs defined according to Coenen et al. [12] to the streamline selection of the slMFB from the whole-brain tractogram in the coronal (B), axial (C) and sagittal (D) planes. *Figure legend: AC: anterior commissure; CC: corpus callosum; CN: caudate nucleus; Fx: fornix; GPe: globus pallidus externus; MB: mamillary body; MTT: mamillothalamic tract; PU: putamen; RN: red nucleus; SN: substantia nigra; STN: subthalamic nucleus; Th: thalamus*

3.4. Individual contributions

The fiber dissections of the subthalamic region, the histological examinations and the tractographies are work of Cintia Mészáros. The fiber dissections of the septum verum are attributed to László Bárány.

DOI:10.14753/SE.2025.3062

4. Results

4.1. Subthalamic region

At the beginning of the dissections, the hypothalamic sulcus coursing on the lateral wall of the third ventricle between the thalamus and the hypothalamus served as a good landmark. The first step of the dissections was the careful removal of the thalamus and the medial part of the hypothalamus, the lateral border of the latter being marked by the column of the fornix and the MTT. The exact boundaries of the subthalamic region were difficult to define from most directions. Its medial border was continuous with the lateral and posterior hypothalamus, while its posterior border with the tegmentum of the mesencephalon. There was no apparent border visible towards the thalamus either. However, its anterior and lateral boundaries were clearly defined by the internal capsule and inferiorly by the transition zone between the crus cerebri and the internal capsule.

The fiber bundle of the MFB visualized and described using tractography [11, 12] was absent in all 19 examined brain hemispheres (100 %) using fiber dissection.

4.1.1. The red nucleus and the fasciculus retroflexus

Due to its fibrous capsule, the red nucleus was relatively well separable from the surrounding structures. Under the most superficial layer of its capsule, the fasciculus retroflexus (habenulointerpeduncular tract) could be identified on its medial surface. This well-defined fiber tract connected the inferior portion of the habenula with the interpeduncular region. The capsule of the red nucleus was predominantly composed of cerebellar fibers, but other fibers from the brainstem also participated in its creation. Most fibers of the nucleus itself and of its capsule ran toward the thalamus composing a part of the thalamic fasciculus. [**Figures 4 and 7**]

DOI:10.14753/SE.2025.3062

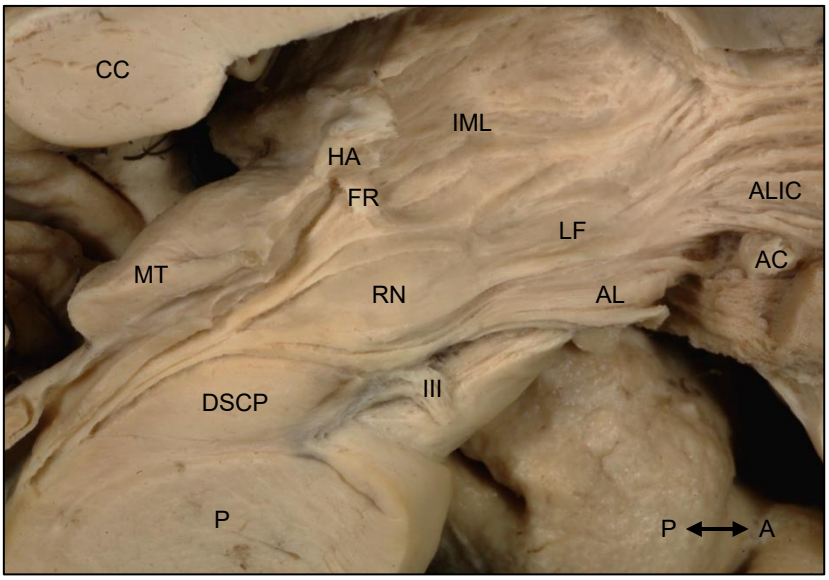

Figure 4 – Fiber bundles after removing the most superficial fibers of the brainstem and the pulvinar of the thalamus.

The initial section of the fasciculus retroflexus inferior to the habenula served as a good orientation point. The distal part of this fiber bundle was covered by the most superficial layer of the capsule of the red nucleus, which consisted of fibers originating from the brainstem. *Figure legend: III: oculomotor nerve; AC: anterior commissure; AL: ansa lenticularis; ALIC: anterior limb of the internal capsule; CC: corpus callosum; DSCP: decussation of the superior cerebellar peduncle; FR: fasciculus retroflexus; HA: habenula; IML: internal medullary lamina of the thalamus; LF: lenticular fasciculus; MT: mesencephalic tectum; P: pons; RN: red nucleus. Compass: A: anterior; P: posterior*

4.1.2. The ansa lenticularis

The ansa lenticularis was recognized as a bundle curving around the cerebral peduncle and running directly lateral to the MTT and the column of the fornix in the lateral hypothalamus. The majority of its fibers originated in the area inferomedial to the red nucleus and anterior to the decussation of the SCP and approached, even intermingled with the fibers of the oculomotor nerve. Rostrally, the fibers of the ansa lenticularis reached the globus pallidus, the ventral pallidum and the substantia innominata. [**Figures 4-8**]

DOI:10.14753/SE.2025.3062

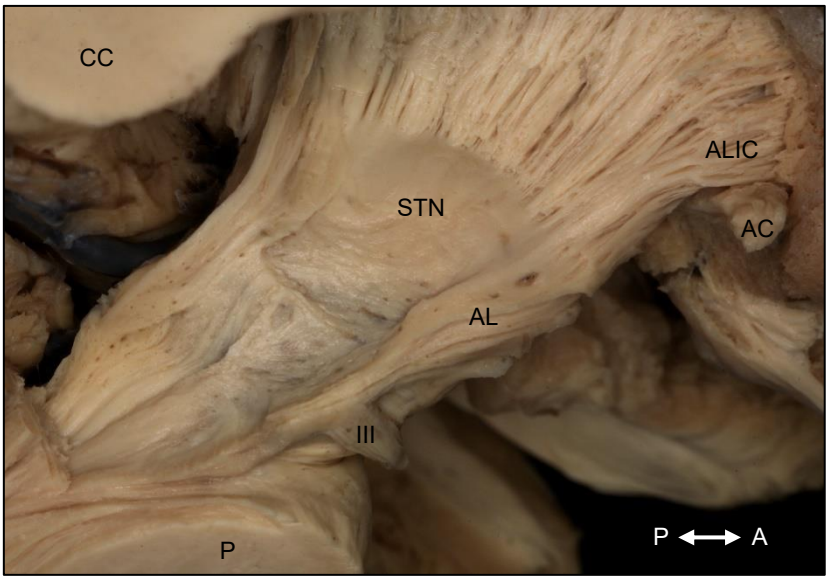

Figure 5 – The relationship of the ansa lenticularis to the oculomotor nerve and the subthalamic nucleus [42]

Most fibers of the ansa lenticularis originated from the area anterior to the decussation of the superior cerebellar peduncle and inferomedial to the red nucleus. The close relationship between the ansa lenticularis and the oculomotor nerve is well visible. *Figure legend: III: oculomotor nerve; AC: anterior commissure; AL: ansa lenticularis; ALIC: anterior limb of the internal capsule; CC: corpus callosum;; P: pons; STN: subthalamic nucleus. Compass: A: anterior; P: posterior*

DOI:10.14753/SE.2025.3062

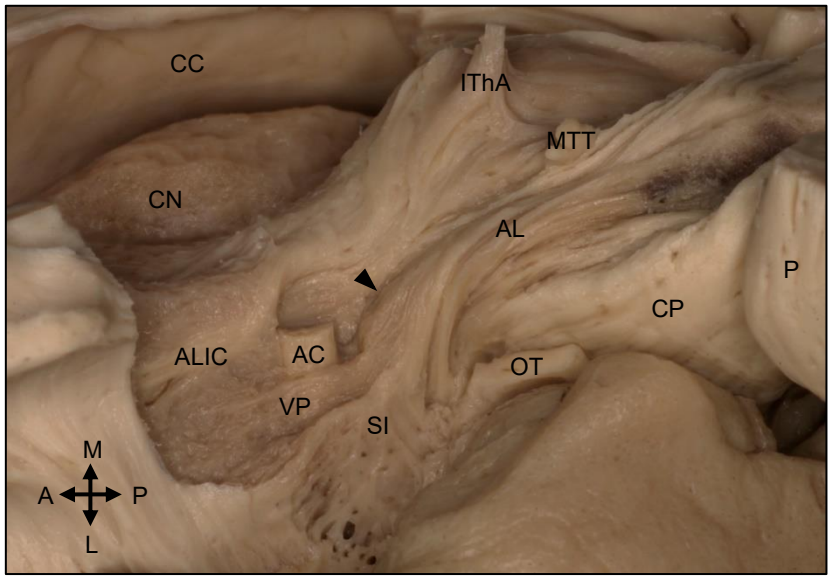

Figure 6 – The course of the ansa lenticularis from an inferomedial aspect [42]
The topographical relationship between the mamillothalamic tract and the ansa lenticularis is well visible. Black arrowhead marks the thin fibers leaving the ansa lenticularis and coursing towards the ventral pallidum and the substantia innominata from the mesencephalon. *Figure legend: AC: anterior commissure; AL: ansa lenticularis; ALIC: anterior limb of the internal capsule; CC: corpus callosum; CN: caudate nucleus; CP: cerebral peduncle; IThA: interthalamic adhesion, MTT: mamillothalamic tract; OT: optic tract; P: pons; SI: substantia innominata; VP: ventral pallidum. Compass: A: anterior; L: lateral; M: medial; P: posterior*

4.1.3. The lenticular fasciculus

The lenticular fasciculus appeared macroscopically as a sheet-like white matter covering the STN and rostral to it the fibers of the internal capsule. It was made up of several thin layers consisting of fibers that traversed the internal capsule to reach the subthalamic region. These fibers initially coursed medially, then made a sharp turn laterally to participate in the formation of the thalamic fasciculus. The medial edge of the lenticular fasciculus directly adjoined the ansa lenticularis and no apparent border could be defined between them until that point where the ansa lenticularis turned around the

DOI:10.14753/SE.2025.3062

cerebral peduncle. The most medial fibers running in the immediate vicinity of the ansa lenticularis were in relationship with the medial lemniscus. [**Figures 4, 7-9**]

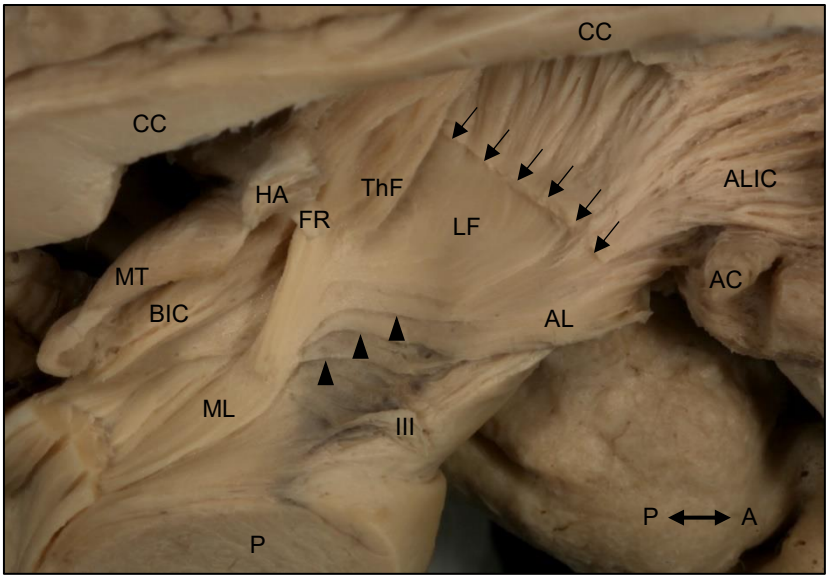

Figure 7 – Fiber systems of the subthalamic region from a medial point of view after removal of the thalamus, the red nucleus, the decussation of the superior cerebellar peduncle and most of the brainstem fibers. [42]

Black arrowheads mark the thin fiber bundles connecting the ansa lenticularis and the lenticular fasciculus to the medial lemniscus running lateral to the red nucleus (already removed). It is well observable that no apparent border can be defined between the ansa lenticularis and the lenticular fasciculus. Black arrows mark the tear line of the most dorsal layers of the lenticular fasciculus just before they pierce the internal capsule. *Figure legend: III: oculomotor nerve; AC: anterior commissure; AL: ansa lenticularis; ALIC: anterior limb of the internal capsule; BIC: brachium of the inferior colliculus; CC: corpus callosum; FR: fasciculus retroflexus; HA: habenula; LF: lenticular fasciculus; ML: medial lemniscus; MT: mesencephalic tectum; P: pons; ThF: thalamic fasciculus. Compass: A: anterior; P: posterior*

DOI:10.14753/SE.2025.3062

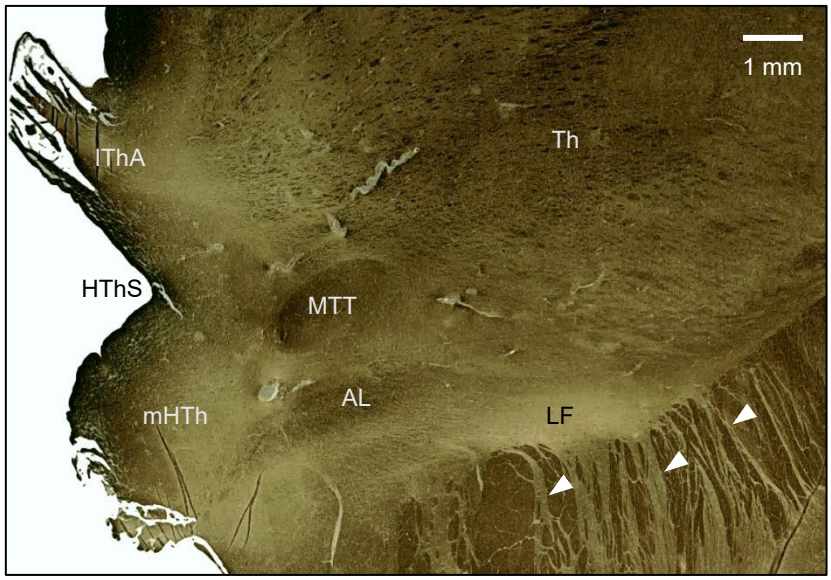

Figure 8 – Histological section in the coronal plane at the level of the interthalamic adhesion showing the relationship of the ansa lenticularis to the mamillothalamic tract and the lenticular fasciculus. [42]

The use of circular polarized light allowed the separation of the ansa lenticularis and the lenticular fasciculus due to their different fiber orientations. The predominantly cross-sectioned ansa lenticularis appears as a darker, while the mainly longitudinal and oblique fibers of the lenticular fasciculus as a brighter layer. The white arrowheads show fiber bundles of the lenticular fasciculus penetrating the internal capsule. Original magnification 4x, stained with neurofibril silver impregnation. The left side of the figure corresponds to the medial direction. *Figure legend: AL: ansa lenticularis; HThS: hypothalamic sulcus; IThA: interthalamic adhesion; LF: lenticular fasciculus; mHTh: medial hypothalamus; MTT: mamillothalamic tract; Th: thalamus*

DOI:10.14753/SE.2025.3062

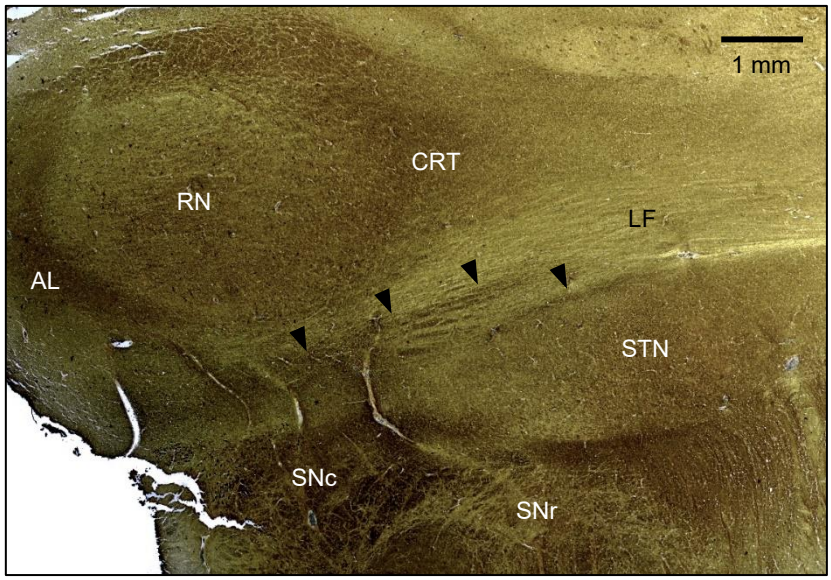

Figure 9 – Coronal section through the rostral part of the red nucleus [42]
The black arrowheads indicate cross-sections of thin fiber bundles connecting the ansa lenticularis and the lenticular fasciculus to the medial lemniscus running on the dorsomedial surface of the subthalamic nucleus (STN) and inferolateral to the red nucleus (see macroscopically in Figure 7). Using circular polarized light, the lenticular fasciculus appears as a bright layer dorsal and lateral to these bundles. The ambiguous medial border of the STN is also well observable. The left side of the figure corresponds to the medial direction. Original magnification 4x, stained with neurofibril silver impregnation. *Figure legend: AL: ansa lenticularis; CRT: cerebello-rubro-thalamic fibers; LF: lenticular fasciculus; RN: red nucleus; SNc: pars compacta of the substantia nigra; SNr: pars reticularis of the substantia nigra; STN: subthalamic nucleus*

4.1.4. The thalamic fasciculus

The thalamic fasciculus was identified as a less defined bundle consisting mainly of bilateral cerebellar fibers as well as fibers from the lenticular fasciculus. It coursed lateral to the red nucleus and the fasciculus retroflexus before it entered the thalamus. Some fibers of the lemniscal system also joined it from the posterior direction. [**Figure 7**]

DOI:10.14753/SE.2025.3062

4.1.5. The subthalamic nucleus

The STN appeared as a lens-shaped grey matter under the caudal portion of the lenticular fasciculus. It was bordered rostrally by the internal capsule and the rostral portion of the lenticular fasciculus, laterally by the internal capsule, caudally by bilateral cerebellar fibers as well as the bundles of the lemniscal system and medially by the lateral hypothalamus and the ansa lenticularis. Its inferior border was the transition zone between the crus cerebri and the internal capsule together with the substantia nigra. Its medial border was continuous with the adjacent hypothalamus and covered by the ansa lenticularis. From this region, a fiber bundle could be followed to the anterior tip of the globus pallidus externus (GPe) as well as towards the PFC through the ALIC running in the most lateral part of the ansa lenticularis. [**Figures 5, 9-11**]

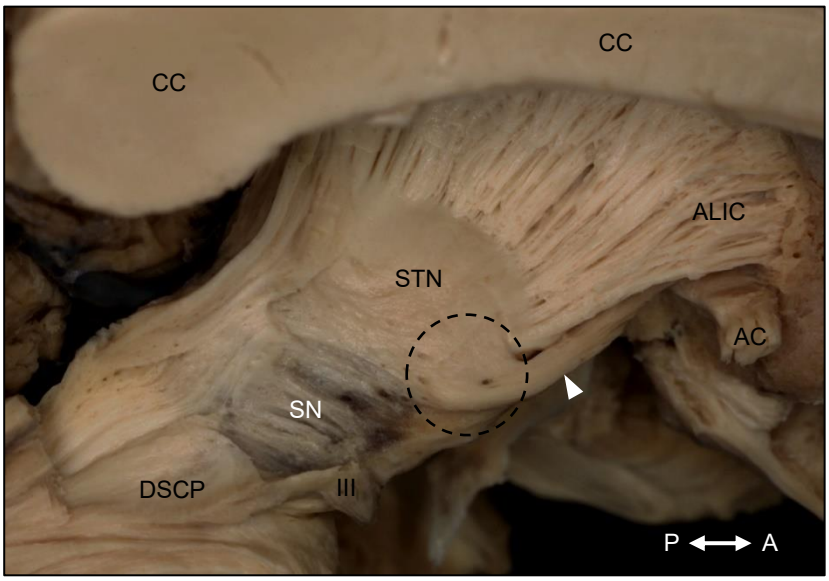

Figure 10 – The subthalamic nucleus (STN) after removal of the thalamus as well as most of the subthalamic and brainstem fibers from a dorsomedial point of view. [42]

The dashed line marks the medial tip of the STN which is continuous with the adjacent hypothalamus. This region corresponds to the limbic cone of the STN. White arrowhead marks the fiber bundle arising from this region and running in the most lateral part of the ansa lenticularis to the anterior tip of the external globus pallidus as well as towards the prefrontal cortex through the anterior limb of the internal capsule. *Figure legend: III: oculomotor nerve; AC: anterior commissure; ALIC: anterior limb of the internal capsule; CC: corpus callosum; DSCP: position of the removed*

decussation of the superior cerebellar peduncle; SN: substantia nigra; STN: subthalamic nucleus. Compass: A: anterior; P: posterior

4.1.6. The substantia nigra

The substantia nigra could be observed as a thin plate of grey matter at the border of the mesencephalic tegmentum and the crus cerebri. Its two parts were clearly distinguishable: the dorsal pars compacta with its typically black color, and the ventral pars reticularis with its reddish-brown color. Its rostral end extended into the subthalamic region ventral to the STN, while its caudal end reached the upper pons. [**Figures 9 and 10**]

4.1.7. The external globus pallidus

Ventral to the anterior commissure, the grey matter of the ventral pallidum was recognizable, where thin fibers running along the ansa lenticularis terminated. The anterior tip of the GPe was visible dorsal to the anterior commissure, directly lateral to the ALIC. In this part of the GPe fibers terminated from the medial tip of the STN initially traveling in the most lateral part of the ansa lenticularis. The globus pallidus did not have an ordinary grey matter appearance due to the many fibers passing through it; therefore, it was difficult to separate it from the adjacent structures. Its close relationship with the ALIC was remarkable, from which it was practically inseparable; the border between them was both macro- and microscopically rather ambiguous. Some fibers could also be observed entering the ALIC from the GPe. [**Figures 11-13**]

DOI:10.14753/SE.2025.3062

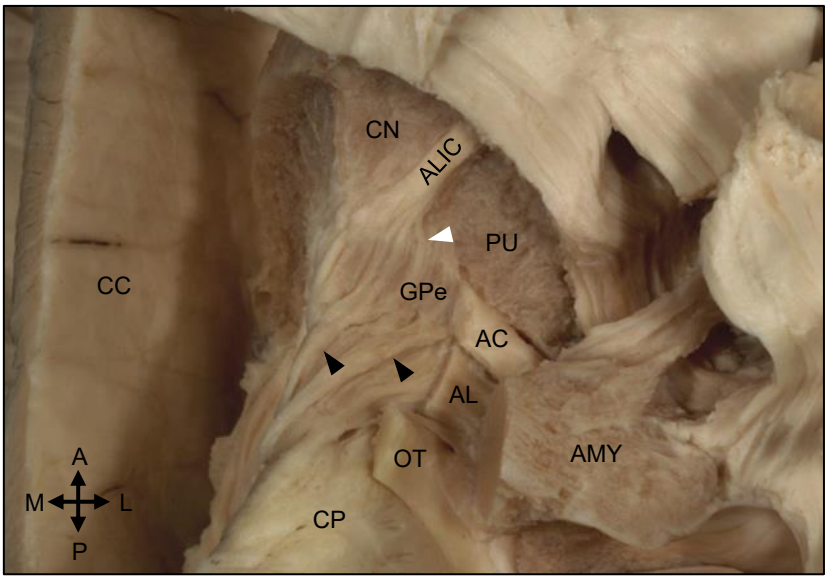

Figure 11 – The relationship between the anterior limb of the internal capsule and the anterior tip of the globus pallidus externus [42]

The black arrowheads indicate fibers originating from the limbic cone of the STN running in the most lateral part of the ansa lenticularis. Fibers entering the ALIC from the GPe are marked with white arrowhead. The ambiguous border between them is well observable. *Figure legend: AC: anterior commissure; AL: ansa lenticularis; ALIC: anterior limb of the internal capsule; AMY: amygdala; CC: corpus callosum; CN: caudate nucleus; CP: cerebral peduncle; GPe: globus pallidus externus; OT: optic tract; PU: putamen. Compass: A: anterior; L: lateral; M: medial; P: posterior*

DOI:10.14753/SE.2025.3062

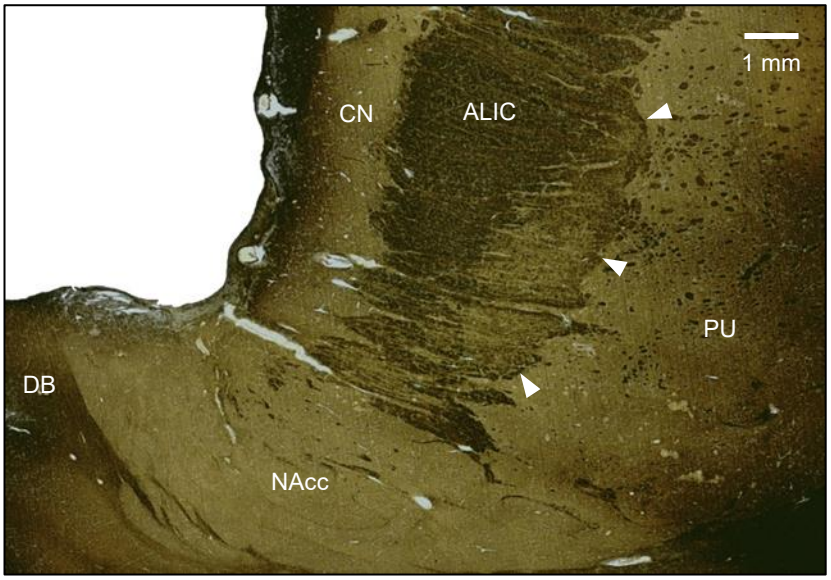

Figure 12 – Coronal section at the level of the nucleus accumbens. [42]

White arrowheads indicate the lateral border of the globus pallidus externus (GPe). Note the close relationship between the ALIC and the anterior tip of the GPe. Original magnification 4x, stained with neurofibril silver impregnation. The left side of the figure corresponds to the medial direction. *Figure legend: ALIC: anterior limb of the internal capsule; CN: caudate nucleus; DB: diagonal band of Broca; NAcc: nucleus accumbens; PU: putamen.*

DOI:10.14753/SE.2025.3062

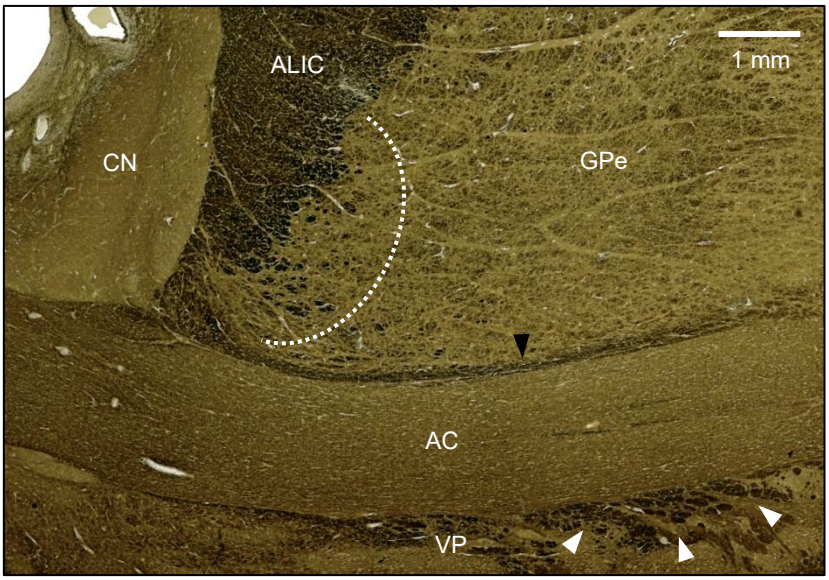

Figure 13 – Coronal section at the level of the anterior commissure. [42]

In the area marked with a white dotted line, fiber exchange between the anterior limb of the internal capsule and the globus pallidus externus can be observed. Gratiolet's canal is marked with a black arrowhead. Ventral to the anterior commissure, white arrowheads indicate cross-sections of fiber bundles corresponding to the thin fibers running along the ansa lenticularis towards the ventral pallidum and the substantia innominata as showed macroscopically in Figure 6. Original magnification 4x, stained with neurofibril silver impregnation. The left side of the figure corresponds to the medial direction. *Figure legend: AC: anterior commissure; ALIC: anterior limb of the internal capsule; CN: caudate nucleus; GPe: globus pallidus externus; VP: ventral pallidum*

4.1.8. Tractography

The results obtained with tractography were notably dependent on the cutoff values, especially when using MSMT-CSD. Streamlines between the ROI defined by Coenen et al. [12] and the PFC traveling through the ALIC could be observed in all cases when using DTI, independent from the FA-threshold. However, using MSMT-CSD, the raising of the FOD threshold caused a strong decrease of the number of streamlines with a similar course. Using the ALIC as a single ROI, the streamlines corresponding to the anterior thalamic radiation as well as Arnold's frontopontine tract were constant findings. Interestingly, the average number of streamlines running through the ALIC increased despite raising the cutoff values, which was accompanied by a reduction in the number of definitely false-positive streamlines (e.g. that belonged to the fornix), especially when using MSMT-CSD. The increase of the FOD cutoff value finally resulted in the elimination of the streamlines corresponding to the slMFB. [**Figures 14, 15 and Table 1**]

DOI:10.14753/SE.2025.3062

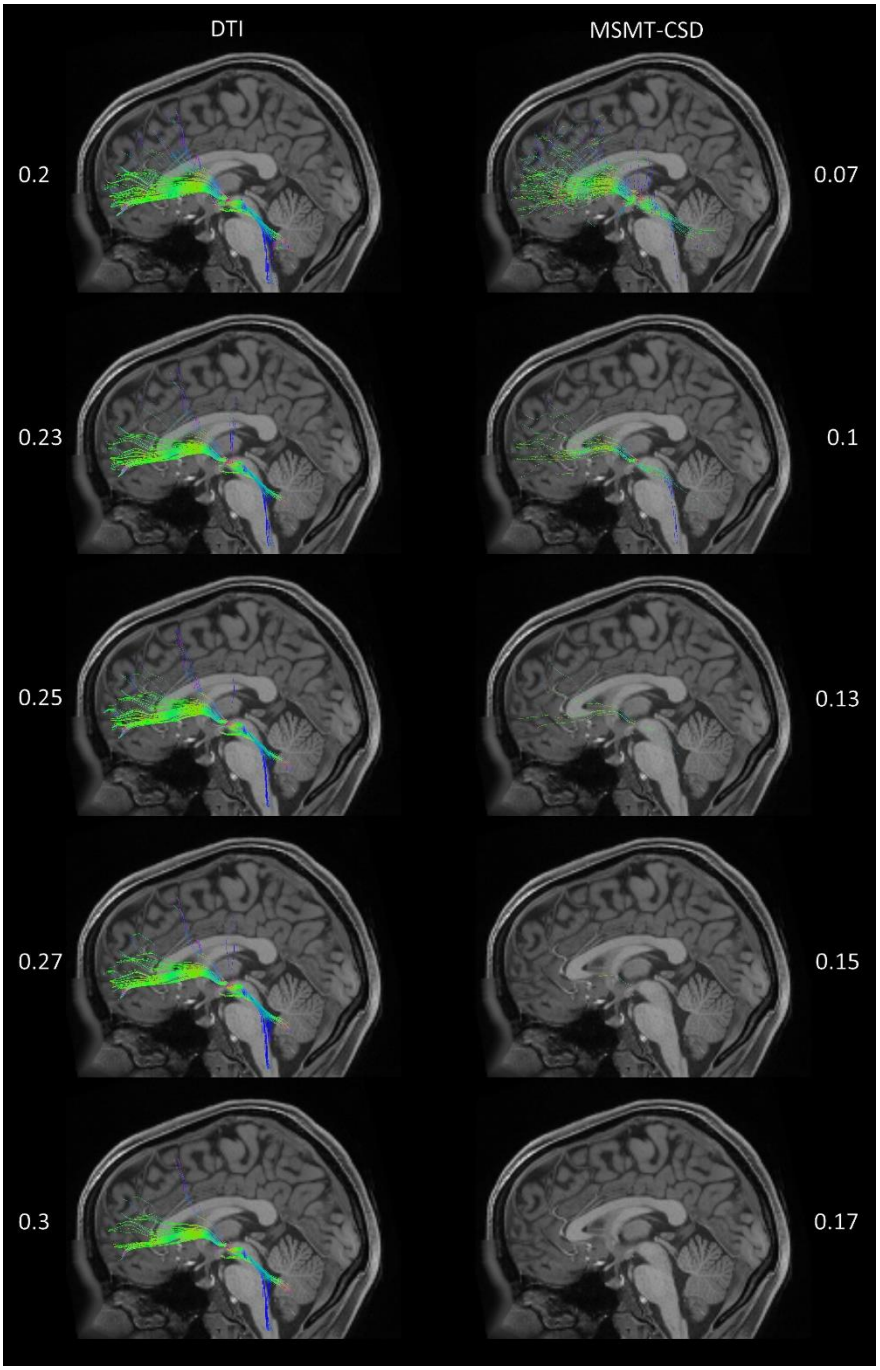

Figure 14 - Tractograms showing the superolateral branch of the medial forebrain bundle (slMFB) isolated from the whole brain tractogram using the region of interests showed in Figure 3. [42]

The left side of the figure shows results obtained with DTI-tractography, depending on the FA threshold. On the right, tractograms obtained using MSMT-CSD-tractography are shown, depending on the FOD threshold. Using DTI, the streamlines corresponding to the slMFB were present almost independently of the FA threshold.

DOI:10.14753/SE.2025.3062

However, they disappeared by increasing the FOD threshold when using MSMT-CSD.

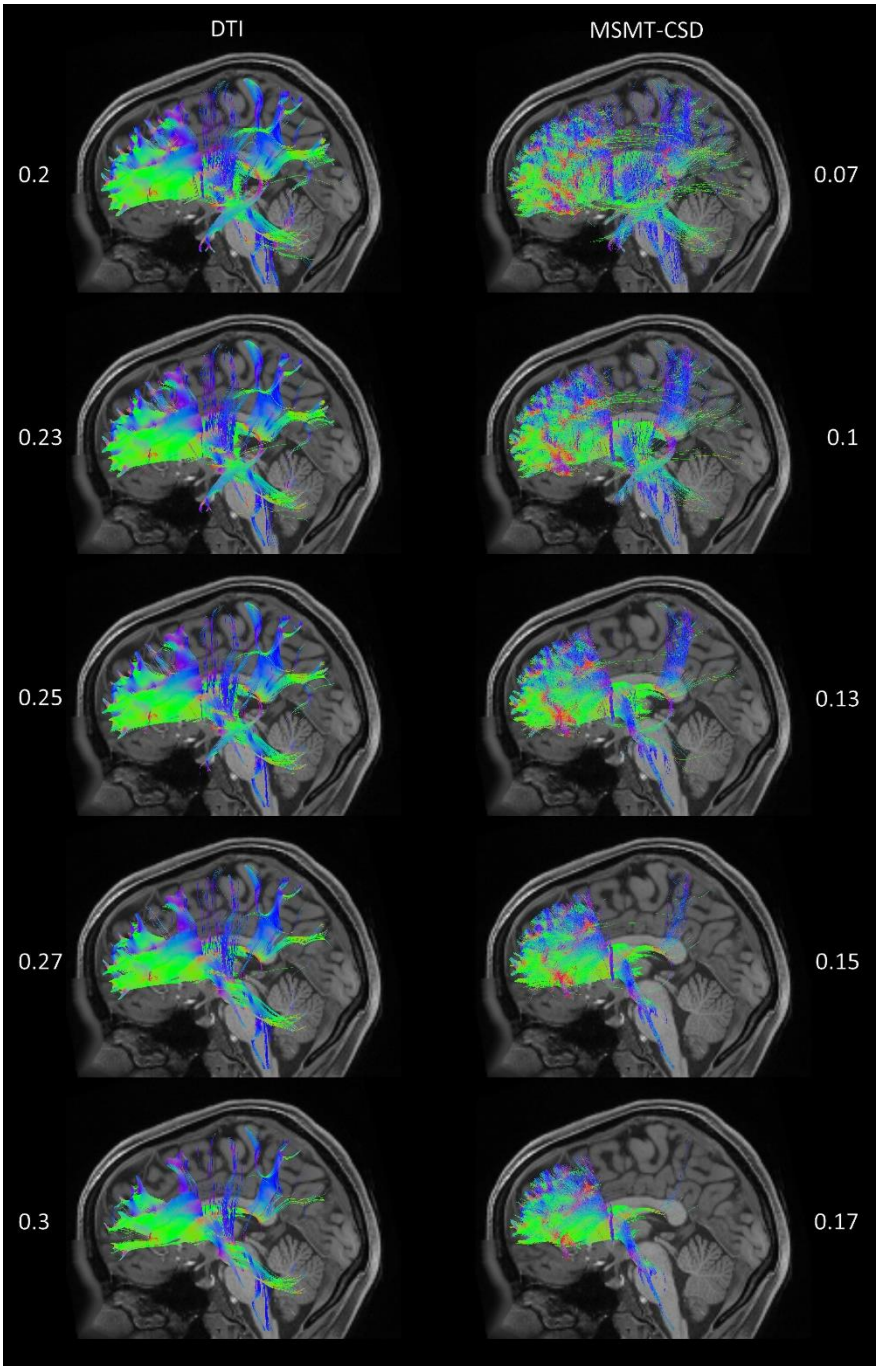

Figure 15 - Tractograms showing the streamlines passing through the anterior limb of the internal capsule (ALIC) isolated from the whole brain tractogram using the region of interest (ROI) showed in Figure 3/A. [42]

DOI:10.14753/SE.2025.3062

Same subject and side as in Figure 14. On the left side, results obtained with DTI-tractography can be seen depending on the FA threshold. On the right side, tractograms obtained using MSMT-CSD-tractography are shown, depending on the FOD threshold. With DTI, very extensive connections can be observed, which hardly changed when the threshold is raised. Streamlines corresponding to the slMFB are also visible. On the other hand, when raising the FOD threshold using MSMT-CSD, the anterior thalamic radiation and frontopontine tract running through the ALIC are more and more clearly represented thanks to the disappearing false-positive streamlines.

Table 1 – Quantitative results obtained with tractography

Average streamline count and proportion of the slMFB streamlines in the ALIC by increasing the cutoff values using DTI- and MSMT-CSD-tractography based on the results obtained from all 200 brain hemispheres.

DTI				MSMT-CSD			
FA threshold	Average streamline count in the ALIC	Average streamline count representing the slMFB	Proportion of the streamlines representing the slMFB running through the ALIC	FOD threshold	Average streamline count in the ALIC	Average streamline count representing the slMFB	Proportion of the streamlines representing the slMFB running through the ALIC
0.2	9594	626	6.35%	0.07	6995	231	3.20%
0.23	10488	612	5.69%	0.1	7609	133	1.68%
0.25	11209	588	5.14%	0.13	8489	56	0.63%
0.27	12032	559	4.57%	0.15	9053	26	0.27%
0.3	13470	499	3.64%	0.17	9528	11	0.10%

DOI:10.14753/SE.2025.3062

4.2. Septum verum

The septum verum composed the ventral part of the medial wall of the lateral ventricle's frontal horn. Macroscopically it was difficult to find a clear boundary between it and the dorsal laying septum pellucidum. Rostrally, it was bordered by the rostrum of the corpus callosum and the anterior parolfactory sulcus, ventrally by the hypothalamus and caudally by the column of the fornix, the anterior commissure and the lamina terminalis. The dorsal part of its lateral surface was covered by ventricular ependyma, while its ventral part was continuous with the grey matter of the nucleus accumbens and the BNST.

4.2.1. The precommissural fornix

The precommissural fibers of the fornix composed the lateral part of the corpus of the fornix and left its main bundle just dorsal to the foramen of Monro. After a short course in anteroinferior direction, they terminated in the septal nuclei rostral to the anterior commissure. A thin grey matter substance corresponding to the most caudal septal nuclei was also observable on the dorsal side of these fibers until the level of the foramen of Monro. [**Figures 16, 17 and 19**]

4.2.2. The fasciculus inferior of the septum pellucidum

These fibers originated from the septal nuclei and intermingled with the terminating fibers of the precommissural fornix. After a straight course in anterosuperior direction they joined the fasciculus superior of the septum pellucidum at the genu of the corpus callosum, then turned lateral and were lost between the fibers of the forceps minor of the corpus callosum. [**Figures 16, 19 and 20**]

DOI:10.14753/SE.2025.3062

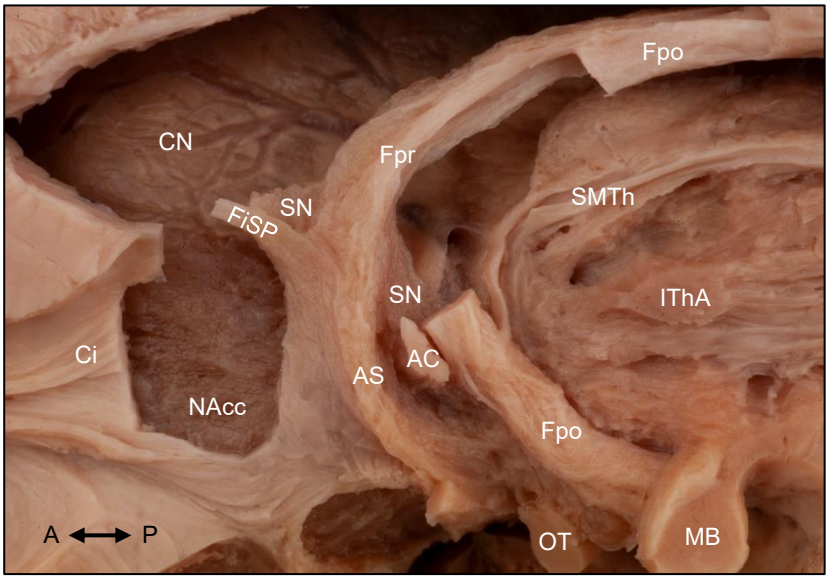

Figure 16 – Topographical relationships of the white matter connections of the septal region after the removal of the septum pellucidum and most of the septal nuclei from a medial point of view.

No apparent border can be seen between the septum verum, the caudate nucleus and the nucleus accumbens. *Figure legend: AC: anterior commissure; AS: amygdaloseptal fibers; Ci: cingulum; CN: caudate nucleus; FiSP: fasciculus inferior of the septum pellucidum; Fpo: postcommissural fornix; Fpr: precommissural fornix; IThA: interthalamic adhesion; MB: mamillary body; NAcc: nucleus accumbens; OT: optic tract; SMTh: stria medullaris of thalamus; SN: septal nuclei. Compass: A: anterior; P: posterior*

4.2.3. The cingulum

The cingulum was a prominent white matter bundle coursing parallel to the dorsal surface of the corpus callosum. Ventral to the genu of the corpus callosum, a fiber bundle was visible connecting the cingulum to the rostral part of the septum verum, just ventral to the fibers of the fasciculus inferior of the septum pellucidum. This bundle was covered medially by the most superficial part of the vertical limb of the diagonal band of Broca. [**Figures 16, 17 and 20**]

DOI:10.14753/SE.2025.3062

4.2.4. The medial olfactory stria

The medial olfactory stria left the olfactory tract just anterior to the anterior perforated substance and coursed in a dorsomedial direction towards the septum verum. Its fibers terminated in the rostral part of the septum verum just posterior to the fibers belonging to the cingulum. [**Figures 17 and 20**]

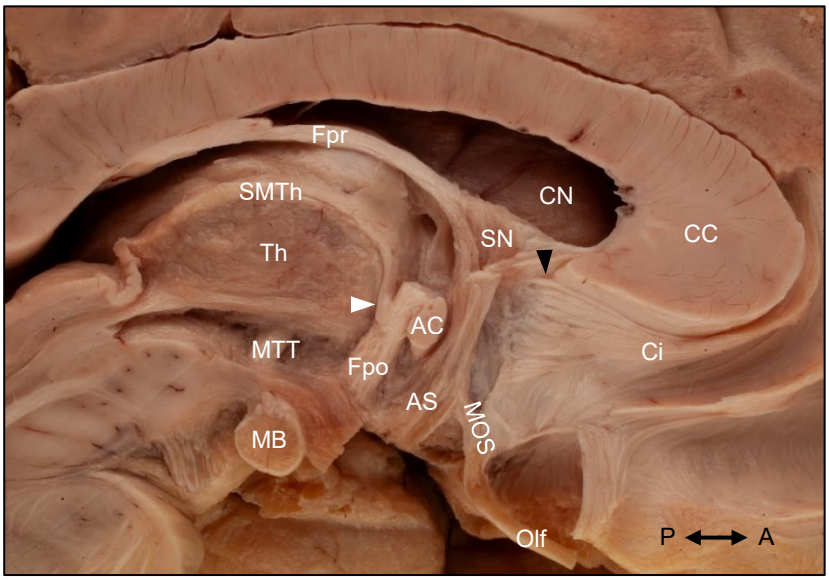

Figure 17 - White matter connections of the septum verum from a medial point of view.

The septum pellucidum, the diagonal band of Broca and the grey matter of the subcallosal area were removed. The fiber bundle connecting the cingulum to the rostral part of the septum verum is indicated with a black arrowhead. White arrowhead marks the connection between the postcommissural column of the fornix and the stria medullaris of thalamus. *Figure legend: AC: anterior commissure; AS: amygdaloseptal fibers; CC: corpus callosum; Ci: cingulum; CN: caudate nucleus; Fpo: postcommissural fibers of the fornix; Fpr: precommissural fibers of the fornix; MB: mamillary body; MOS: medial olfactory stria; MTT: mammillothalamic tract; Olf: olfactory tract; SMTh: stria medullaris of thalamus; SN: septal nuclei; Th: thalamus. Compass: A: anterior; P: posterior*

DOI:10.14753/SE.2025.3062

4.2.5. The ventral amygdalofugal pathway

After removing the grey matter of the diagonal band of Broca, the amygdaloseptal fibers connecting the ipsilateral amygdala to the septal nuclei became visible. This pathway consisted of a horizontal and a vertical limb. Its horizontal limb could be observed on the basal surface of the brain and ran parallel and ventral to the anterior commissure. Directly caudal to it, the inferior thalamic peduncle containing the amygdalothalamic and amygdalohypothalamic fibers could be observed. The vertical part of the amygdaloseptal fibers coursed on the medial surface of the brain through the paraterminal gyrus and a part of this bundle joined the subgenual cingulum. [**Figures 16-18, 20, 22 and 23**]

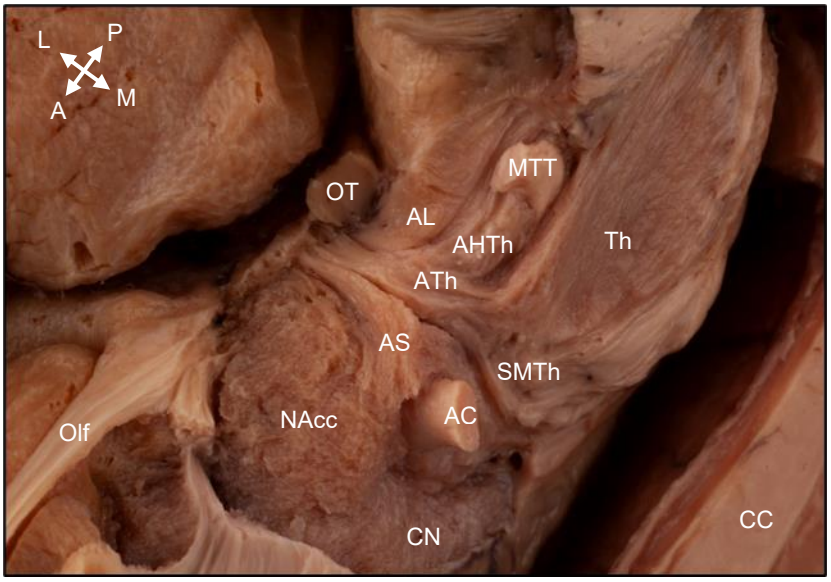

Figure 18 – Fiber connections coursing through the basal forebrain from a mediobasal point of view.

The diagonal band of Broca containing the amygdaloseptal fibers run just anterior to the amygdalothalamic fibers to the septal nuclei. *Figure legend: AC: anterior commissure; AHTh: amygdalohypothalamic fibers; AL: ansa lenticularis; AS: amygdaloseptal fibers; ATh: amygdalothalamic fibers; CC: corpus callosum; CN: caudate nucleus; MTT: mamillothalamic tract; NAcc: nucleus accumbens; Olf: olfactory tract; OT: optic tract; SMTh: stria medullaris of thalamus; Th: thalamus. Compass: A: anterior; L: lateral; M: medial; P: posterior*

DOI:10.14753/SE.2025.3062

4.2.6. The stria medullaris of thalamus

The main bundle of the SMTh could be seen coursing between the posterior border of the interventricular foramen and the ipsilateral habenula along the border of the medial and dorsal surface of the thalamus. Some fibers of it crossed the midline through the habenular commissure and the interthalamic adhesion. Thalamohabenular fibers were also constant findings connecting the anterior thalamic nuclei and the habenula.

An interesting observation of this study was that a significant amount of fibers left the postcommissural column of the fornix at the beginning of its pars tecta and connected it to the ipsilateral SMTh as well as the anterior nuclei of the ipsilateral thalamus. These bundles could be observed in all cases at the level of the anterior commissure as they leave the column of the fornix and made a short hairpin-like turn along the inferior border of the interventricular foramen. The fibers running to the SMTh and the thalamus formed either a common bundle or the ones coursing to the thalamus left the postcommissural fornix a few millimeters distal to the fibers connecting it to the SMTh. [**Figures 16-23**]

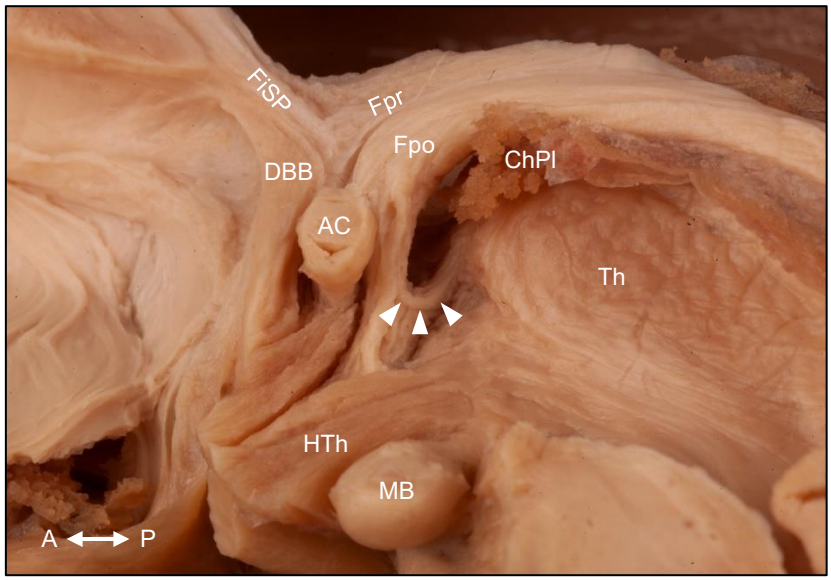

Figure 19 – The region of septum verum before the removal of the diagonal band of Broca.

The hairpin-like course of the fibers connecting the postcommissural column of the fornix to the stria medullaris of thalamus is well visible (white arrowheads). *Figure legend: AC: anterior commissure; ChPl: choroid plexus; DBB: diagonal band of Broca; FiSP: fasciculus inferior of the septum pellucidum; Fpo: postcommissural*

DOI:10.14753/SE.2025.3062

fibers of the fornix; Fpr: precommissural fibers of the fornix; HTh: hypothalamus; MB: mamillary body; Th: thalamus. Compass: A: anterior; P: posterior

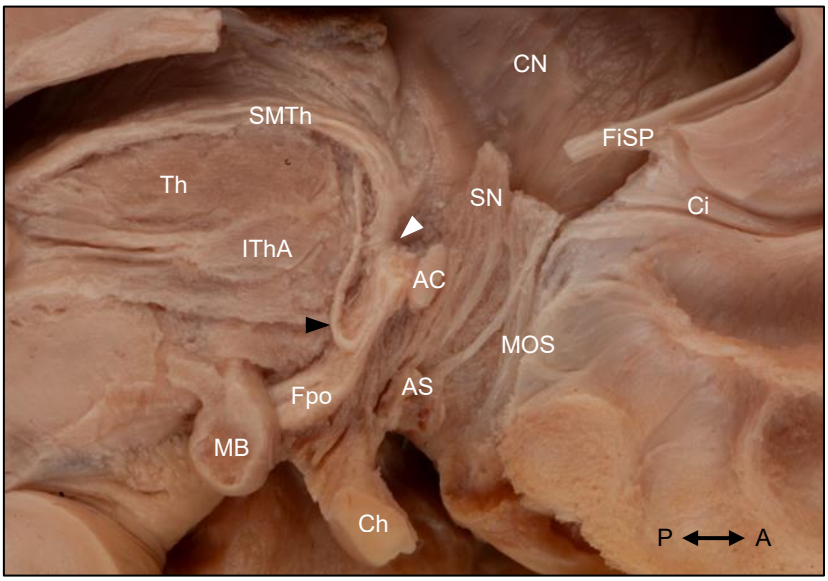

Figure 20 – The fiber connections of the septum verum after the removal of the diagonal band of Broca.

Removing the ependyma covering the medial surface of the thalamus as well as a part of the medial hypothalamus revealed the fiber bundle connecting the postcommissural column of the fornix to the anterior thalamic nuclei (black arrowhead). Just proximal to it, the connection with the stria medullaris of thalamus is also visible (white arrowhead). *Figure legend: AC: anterior commissure; AS: amygdaloseptal fibers; Ch: optic chiasm; Ci: cingulum; CN: caudate nucleus; FiSP: fasciculus inferior of the septum pellucidum; Fpo: postcommissural fibers of the fornix; IThA: interthalamic adhesion; MB: mamillary body; MOS: medial olfactory stria; SMTh: stria medullaris of thalamus; SN: septal nuclei; Th: thalamus. Compass: A: anterior; P: posterior*

DOI:10.14753/SE.2025.3062

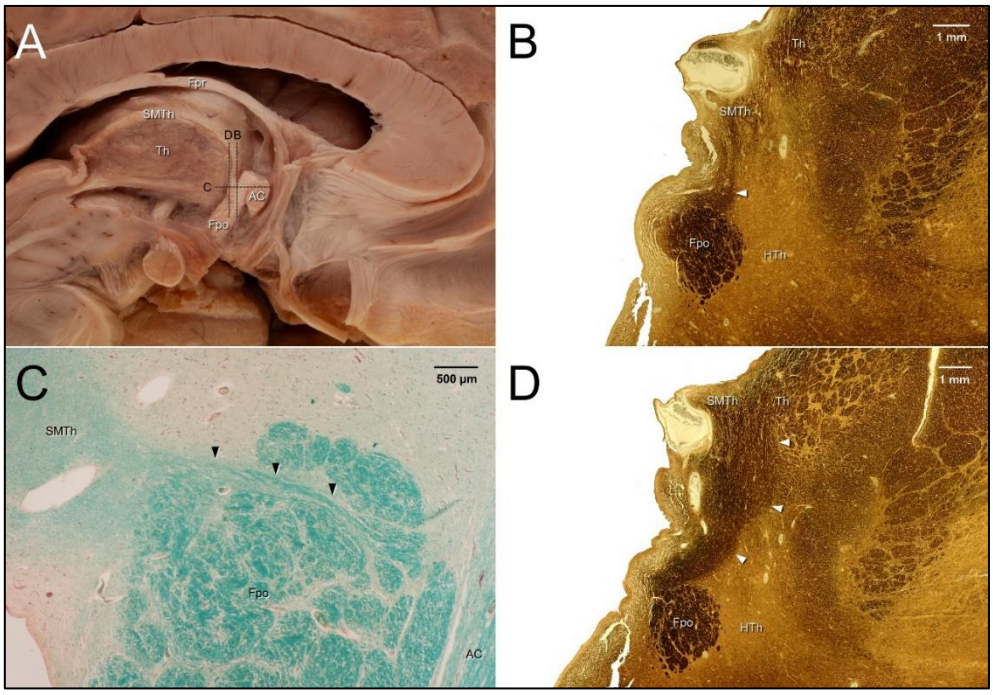

Figure 21 – Histological validation of the fiber connections between the postcommissural column of the fornix and the stria medullaris of thalamus (SMTh) as well as the anterior thalamic nuclei.

Panel A: The plane and localization of the histological sections are indicated with dashed lines. Panel B: white arrowhead marks the connection between the postcommissural fornix and the SMTh. Stained with silver impregnation, original magnification 5x. Panel C: black arrowheads indicate the connecting fibers between the postcommissural fornix and the SMTh in the horizontal plane at the level of the anterior commissure. Stained with Luxol fast blue combined with Sirius red, original magnification 20x. Panel D: White arrowheads mark the fibers leaving the postcommissural fornix and joining the stria medullaris or terminating in the thalamus. Stained with silver impregnation, original magnification 5x. *Figure legend: AC: anterior commissure; Fpo: postcommissural fibers of the fornix; Fpr: precommissural fibers of the fornix; HTh: hypothalamus; SMTh: stria medullaris of thalamus; Th: thalamus*

DOI:10.14753/SE.2025.3062

4.2.7. The stria terminalis

The stria terminalis representing the dorsal amygdalofugal pathway coursed in the sulcus between the caudate nucleus and the thalamus as part of the inferolateral border of the lateral ventricle's pars centralis and connected the amygdala with various regions. The distal part of this bundle was revealed by the careful removal most of the septum verum and the postcommissural fornix. The terminating fibers of the stria terminalis could be divided in nuclear, precommissural and postcommissural components. Most of its fibers terminated in the BNST, a triangular-shaped grey matter structure located directly lateral to the septum verum and just dorsal to the anterior commissure. The removing of this nucleus revealed the postcommissural fibers of the stria terminalis reaching the anterior hypothalamic area. Some of these fibers intermingled with the postcommissural fornix and the proximal fibers of the SMTh. The precommissural portion of the stria terminalis coursed just anterior to the BNST and terminated on the medial side of the nucleus accumbens, rostral to the anterior commissure. [**Figures 22 and 23**]

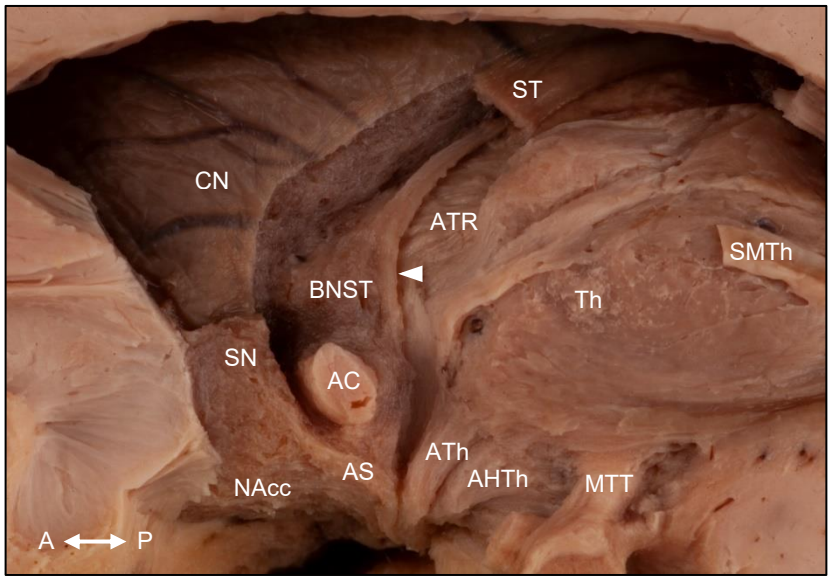

Figure 22 – Deeper layer of the connections of the septum verum from medial.

White arrowhead indicate the nuclear component of the stria terminalis terminating in the bed nucleus of the stria terminalis. *Figure legend: AC: anterior commissure; AHTh: amygdalohypothalamic fibers; AS: amygdaloseptal fibers; ATh: amygdalothalamic fibers; ATR: anterior thalamic radiation; BNST: bed nucleus of the stria terminalis; CN: caudate nucleus; MTT: mammillothalamic tract; NAcc:*

DOI:10.14753/SE.2025.3062

nucleus accumbens; SMTh: stria medullaris of thalamus; SN: septal nuclei; ST: stria terminalis; Th: thalamus. Compass: A: anterior; P: posterior

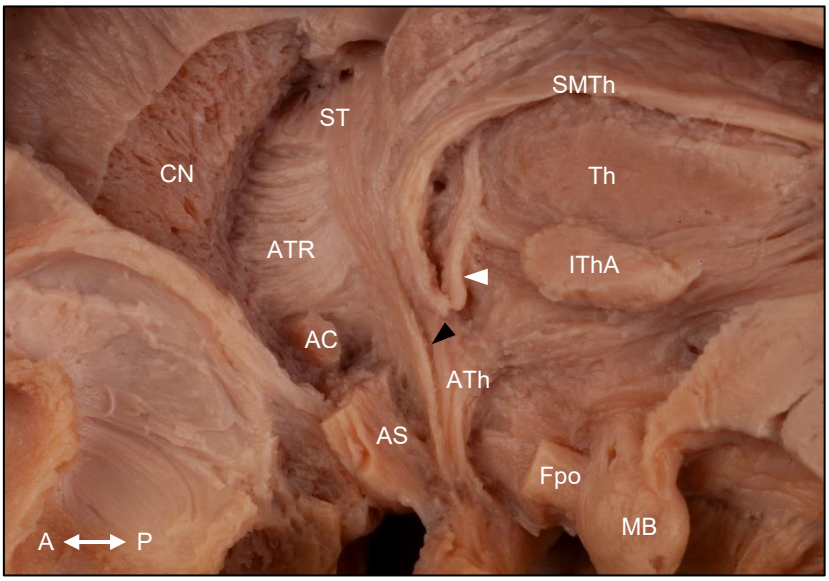

Figure 23 – Removing the bed nucleus of the stria terminalis the postcommissural fibers of the stria terminalis coursing to the hypothalamus became visible (black arrowhead).

White arrowhead indicate the fiber bundle between the stria medullaris thalami and the anterior thalamic nuclei. *Figure legend: AC: anterior commissure; AS: amygdaloseptal fibers; ATh: amygdalothalamic fibers; ATR: anterior thalamic radiation; CN: caudate nucleus; Fpo: postcommissural fibers of the fornix; IThA: interthalamic adhesion; MB: mamillary body; SMTh: stria medullaris of thalamus; ST: stria terminalis; Th: thalamus. Compass: A: anterior; P: posterior*

DOI:10.14753/SE.2025.3062

5. Discussion

5.1. The subthalamic region

The fiber dissections revealed an important difference regarding the course of the ansa lenticularis compared to the original descriptions of the subthalamic region based on Forel's and later Dejerine's histological observations. [4,5] Although this fiber bundle ran through the basal forebrain region indeed and curved around the cerebral peduncle, it did not participate in the formation of the thalamic fasciculus. Additionally, the MFB could not been distinguished as a separate bundle in any of the investigated cases neither macroscopically nor microscopically. Interestingly, most fibers running along the ansa lenticularis exactly mirrored the course of the MFB known from its classical descriptions. [6, 7] Some fibers of it connected midline regions of the lower midbrain/upper pons (presumably the raphe nuclei) and the substantia nigra with basal forebrain regions such as the ventral pallidum and the substantia innominata, but the largest part of it was associated to the area inferomedial to the red nucleus and anterior to the decussation of the SCP. This latter region corresponds to the VTA [43], a dopaminergic territory of the brainstem, which is considered to play an important role in limbic functions. [6, 7]

Both dissection and histological control revealed that the ansa lenticularis pass on the lateral aspect of the MTT through the lateral hypothalamus, reflecting the course of the MFB described in the classical literature. [6, 7] Thin fiber bundles of the ansa lenticularis and lenticular fasciculus were also revealed caudally joining the medial lemniscus. These fibers ran in the posterior subthalamus, ventrolateral to the red nucleus and ventral to the cerebello-rubro-thalamic tract, but their exact origin and termination could not be determined using fiber dissection or histology. The summary of the results obtained with fiber dissection is shown on a schematic diagram in **Figure 24.**

DOI:10.14753/SE.2025.3062

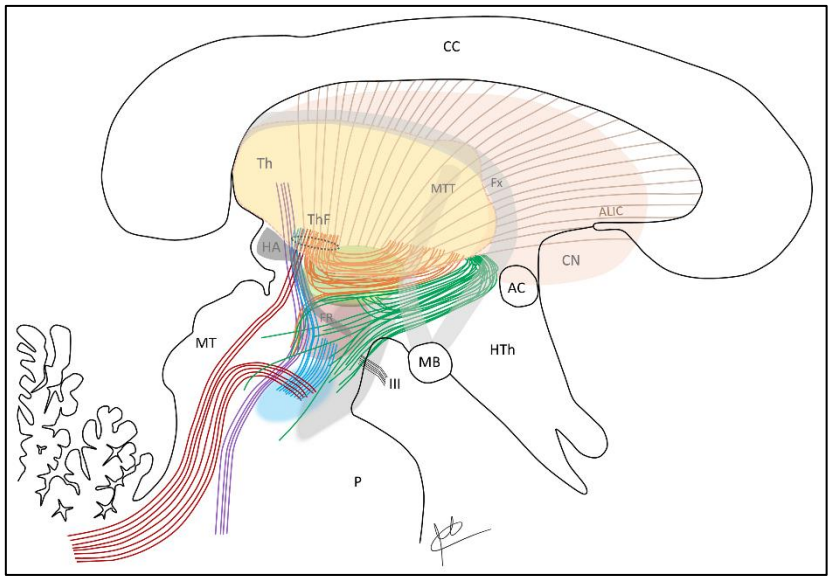

Figure 24 - Schematic diagram showing the fiber connections of the subthalamic region based on the results of the fiber dissections. [42]

The thalamic fasciculus is encircled with a dotted line. *Figure legend: Colored areas: green: subthalamic nucleus; red: red nucleus; blue: decussation of the superior cerebellar peduncle; grey: substantia nigra. Fiber tracts: orange: lenticular fasciculus; green: ansa lenticularis; blue: contralateral cerebellar fibers; red: ipsilateral cerebellar fibers; purple: medial lemniscus. III: oculomotor nerve; AC: anterior commissure; ALIC: anterior limb of the internal capsule; CC: corpus callosum; CN: caudate nucleus; FR: fasciculus retroflexus; Fx: fornix; HA: habenula; HTh: hypothalamus; MB: mamillary body; MT: midbrain tectum; MTT: mamillothalamic tract; P: pons; Th: thalamus; ThF: thalamic fasciculus*

According to Nieuwenhuys et al., the bundle of the MFB running through the lateral hypothalamus separates into a medial and a lateral stream at the diencephalic-mesencephalic junction. [7] The medial stream may be equivalent to the fibers originating in midline brainstem regions such as the VTA, while the latter described thin bundles may represent the lateral stream temporarily joining the medial lemniscus to reach the monoaminergic cell groups in the caudal brainstem. The results of the fiber dissections suggest that most of the monoaminergic fibers corresponding to the rodent MFB join the ansa lenticularis in humans. Tracing experiments in monkeys [44] and immunohistochemical findings in monkey and human brain [45–48] support this theory.

The MFB is well-described in rodents as a loosely arranged fiber bundle running through the lateral hypothalamus, but its course in the human brain is still contradictory.

The first description of this pathway in humans was published using deterministic DTI-tractography. [11, 12] According to the findings of Coenen et al., the human MFB follows a different course as described in rodents and consists of two branches. One part of it was called the imMFB and according to their explanation, it is equivalent to the rodent MFB and runs in a longitudinal direction along the lateral wall of the third ventricle. The second branch, which they named slMFB leaves the latter fiber stream in the region of the VTA and runs more laterally through the subthalamic region to pass through the ventro-lateral part of the ALIC towards the PFC. [11, 12] Since their study, numerous similar results have been published obtained with tractography. [13–20] However, some authors did not agree with this slMFB-concept. In the studies of Haynes and Haber [49] and Haber et al. [50, 51] they performed tract tracing studies and dMRI-tractography on non-human primates as well as human dMRI examinations. Using tract tracing they found that the MFB does not pass through the ALIC, but reaches the PFC ventral to the anterior commissure. In contrast, they obtained similar results as Coenen et al. [12, 50] using dMRI-tractography. The term of slMFB has also been repeatedly criticized, since it considerably differs from the MFB described originally in rodents. Therefore, it was later referred to as the projection pathway of the VTA (VTApp). [50, 52]

According to the findings presented in this thesis, the caudal part of the streamlines described by Coenen et al. corresponds to the ansa lenticularis as well as the lenticular fasciculus. These tracts run in close proximity to each other and because of this, it is likely that the fiber tracking methods cannot surely depict them as separate bundles. Moreover, the fibers of the lenticular fasciculus pierce the internal capsule at the anterior border of the subthalamic region and their fibers intermingle extensively in this region, which is also problematic by the accurate depiction of them by using tractography. Haber et al. found in their immunohistochemical study of non-human primates that a number of monoaminergic fibers leaving the VTA cross the internal capsule to reach the striatum (the fiber dissections revealed that these fibers likely join the lenticular fasciculus). They also claimed that this crossing represents a challenge in the accurate depiction of these fibers using dMRI-tractography, which results in false-positive streamlines coursing through the internal capsule to the PFC. [50, 51] It is well-known that tractography suffers limitations in the correct mapping of such areas with crossing and kissing fibers as well as in “bottleneck” regions. [53] These limiting factors occur cumulatively in the

subthalamic region. Therefore, in this study also a higher-order fiber tracking method was used beyond DTI. The MSMT-CSD tractography allows namely more precise fiber orientation estimation than the diffusion tensor model. [40] Using MSMT-CSD, it was not possible to obtain a uniform tractogram representing the slMFB. The streamline count as well as the proportion of streamlines in the ALIC corresponding to the slMFB strongly decreased with the raising of the FOD cutoff value (see **Table 1**). Interestingly, the average number of streamlines running through the ALIC increased despite raising the cutoff values, which was accompanied with the reduction of definitely false-positive streamlines (e.g. those representing the fornix) by visual control and finally resulted in a complete elimination of the slMFB as well. Along with the findings of the fiber dissections, these results also suggest that the streamlines of the slMFB are in fact false-positive streamlines and they are only a product of the limitations of DTI-tractography.

However, several studies report positive therapeutic effects of slMFB DBS, typically in TRD [54] and OCD [26] when electrodes are implanted direct rostral to the red nucleus to stimulate the slMFB. [13] According to the fiber dissections carried out in this study, the most prominent structure of this region is the ansa lenticularis and most likely the activation of the monoaminergic fibers running along it is responsible for the therapeutic effect. Moreover, the most common side effects during slMFB DBS are oculomotor symptoms, which are also utilized for intraoperative identification of correct electrode position. [13, 25] The close, intermingling relationship between the ansa lenticularis and the exiting fibers of the oculomotor nerve explains this phenomenon.

Another important observation of this study was that the medial tip of the STN was continuous with the lateral hypothalamus both macro- and microscopically which contradicts the latest findings of Coenen et al. obtained with tracing studies of the marmoset brain. [55] Forel and Dejerine already noted that the medial border of this nucleus is rather ambiguous. [4, 5] Results of Haynes and Haber suggested that the medial part of the STN extends into the lateral hypothalamus and this region has a number of limbic connections with the PFC (limbic cone of the STN). [49] Moreover, a recent study emphasized that the STN originates from the hypothalamus during ontogeny and is actually a part of the posterior hypothalamic region. [56] The incomplete separation of these two structures during development can be a possible explanation for the ambiguous border between them. Our anatomical findings support the existence of the limbic cone

region of the STN. We found a number of fibers originating from this region and coursing initially along the ansa lenticularis to the anterior tip of the GPe and through the ALIC towards the PFC. Moreover, we observed fibers entering the ALIC from the GPe which likely predicts that this part of the basal ganglia provides a connection between the limbic cone of the STN and the PFC. It has already been adressed that the globus pallidus has a role not only in motor circuits, but also in limbic and associative functions. [57] In the case study of Saad et al. they observed cognitive and behavioral impairments without motor symptoms in a young patient due to calcification of the anterior part of the GPe. [58] Adler et al. also identified the role of the GPe in behaviour, presumably in the reward circuitry, in a stimulation experiment on a monkey. [59] Furthermore, Baumann et al. found reduced GPe volume in patients with history of affective disorders, compared to healthy control subjects. [60] Our results also support these findings and accordingly it is likely that the GPe could also be a suitable target of DBS in the treatment of TRD. [59]

5.2. The septum verum

According to the description of Andy and Stephan, most of the septal nuclei found in animals are well developed also in humans, only the caudal group is mostly absent or at least significantly regressed. The main difference compared to the septal region of lower animals is the appearance of the septum pellucidum, due to which the septal nuclei of the human brain are elongated in the vertical direction. Andy and Stephan distinguished two parts of the human septum: the septum pellucidum and the septum verum. [27] However, these two parts cannot be sharply demarcated macroscopically, since a part of the septal nuclei is located in the ventral part of the septum pellucidum, and the precommissural fornix - which is one of the most robust connections of the septum verum - also courses through it. [61] Horvath and Palkovits obtained similar results regarding the structure of the human septum, but they used a simplified division, separating the medial and lateral nuclear groups. They also distinguished the nucleus triangularis described as underdeveloped by Andy and Stephan, although they also noted that compared to the size of the whole septum, it is smaller in humans than in rats. Another relevant difference is that the BNST belonging to the caudal nuclear group according to Andy and Stephan was no longer classified as a septal nucleus by them. [28]

The connections of the septum verum in humans have been depicted only in a few dMRI-studies so far and with varying success. The SMTh was first visualized by Kochanski et al. [62] and later by Roddy et al. [63] using tractography. However, they did not describe the connection between the SMTh and the postcommissural fornix dissected in this study, nor the crossing fibers of the SMTh through the interthalamic adhesion. Probably the size of these structures already exceeds the resolution of the fiber tracking method. Kwon et al. depicted the stria terminalis for the first time with tractography, but they could visualize only its hypothalamic (postcommissural) component. [64] Later, Kamali et al. successfully depicted the pre- and postcommissural parts of the stria terminalis with high-resolution tractography. They also described an extension of the precommissural fornix to the medial temporal lobe [65] however, these fibers could not been distinguished during fiber dissections. Li et al. also aimed the visualization of the stria terminalis and other amygdalofugal fibers by tractography. They could find only the nuclear component of this bundle, but they successfully depicted the

amygdaloseptal fibers. [66] Our dissections could reveal all the subcomponents of the stria terminalis described by Klingler and Gloor, except the commissural component. However, they also found these fibers only occasionally in their material. [67] Based on our fiber dissections, the fasciculus inferior of the septum pellucidum along with a bundle of the cingulum also originates in the septum verum. The fasciculi of the septum pellucidum were first visualized using track-density imaging (TDI) by Cho et al. [68] however, to date only the fasciculus superior was further investigated by them, and they concluded that it is most likely a connection between the fornix and the PFC. [69] Based on our current and previous [61] results, the fasciculus inferior of the septum pellucidum approaches, probably also intermingles with the fibers of the fasciculus superior, turns laterally and then joins the fibers of the corpus callosum and presumably - similar to the fasciculus superior - travels to the PFC via the forceps minor. Thus, the fasciculus inferior of the septum pellucidum may also be a connection between the septum verum and the PFC, but further studies are needed to confirm this assumption.

During the fiber dissections of the septal region, a less-known and -accepted connection between the postcommissural column of the fornix and the SMTh was also revealed, which was confirmed by histological validation as well. A macroscopic representation of this connection could only be found in the atlas of Pernkopf, in which it was designated as the hippocampo-habenular tract. [70] Based on careful review of the literature, it is a very controversial relationship, both in terms of its existence and the origin or termination of its fibers. In addition to the name ‘hippocampo-habenular tract’, it can also be found as the (medial) cortico-habenular tract, but most often it was simply referred to as the fibers connecting the postcommissural fornix to the SMTh. All information available about this structure in the literature was based on histological observations. First Gudden mentioned in his comparative study a fiber bundle leaving the fornix ("lateral uncrossed bundle of the fornix"), which, according to him, is connected to the stratum zonale of the thalamus and degenerates when the ipsilateral Ammon's horn is removed. Based on his observations, however, the SMTh only crosses the column of the fornix, without fiber exchange between them. [71] Honegger clearly stated that the column of the fornix sends a bundle of fibers to the SMTh in both animals and humans and in the human brain a particularly compact bundle can be observed. [72] Lotheissen and Kölliker also confirmed its existence. [73, 74] However, Edinger and Wallenberg

categorically rejected the presence of the cortico-habenular tract based on their observations in reptiles, amphibians, and birds [75], as did Cajal. [76] Humphrey described the connection in bats but could not determine its relationship to the hippocampus. [77] Young found this structure in rabbit [78] and Marburg confirmed its existence also in the human brain. [79] In the following years, several lesion studies were published in this regard. Sprague and Meyer observed no degeneration of the SMTh in rabbits with hippocampal lesions. [80] Nauta and Raisman detected degenerating fibers in the SMTh and habenula after lesion of the septal region in rats, but not in the case of hippocampal lesion. [81, 82] In his lesion study of rats, Guillery described fibers coursing from the fornix to the SMTh, but they did not join the SMTh, but ran caudally from it and terminated in the thalamus. [83] Based on their investigations of rats, rabbits and monkeys, Powell and Cowan found that even by complete bilateral lesion of the fornix an intact fiber bundle coming most likely from the septum always remains, the course of which corresponds to the previously described medial cortico-habenular tract and is visible only up to the crossing of the fornix with the SMTh. However, they could not further specify its termination and assumed that either it joins the SMTh, or the fibers are lost in the parataenial nucleus of the thalamus, perhaps in the hypothalamus. [84] The quantitative study of Powell et al. shows that only approximately half of the fibers coursing in the initial part of the postcommissural fornix reaches the mamillary bodies in humans, thus a significant number of fibers must leave it between these two points. They observed that this fiber loss is most gradual in humans, with fibers leaving the fornix along the entire length of the hypothalamus. According to their opinion, the fiber bundle originally described as the medial cortico-habenular tract consists of hippocampo-thalamic and septo-thalamic fibers. [85] Valenstein and Nauta found in their comparative study in rats, hamsters, cats and monkeys that septal fibers run through the fornix to the habenula and the anterior thalamus, but they could only prove the existence of some hippocampo-habenular fibers in hamsters. However, they observed that compared to the other examined animals, the bundle of fibers connecting the fornix to the thalamus is highly developed in monkeys, and in the case of a septal lesion, they observed the greatest degree of SMTh and habenula degeneration in this animal. [86] The lesion study of monkeys of Votaw and Lauer showed that the habenula receives bilateral fibers from Ammon's horn via the fornix and SMTh and there is a homolateral connection between

Ammon's horn and the septum. [87] Based on the literature, it is well visible that the existence and origin of this connection as well as its termination are very contradictory, and it is very likely that there are also interspecies differences. It is assumable that this bundle may contain fibers of both septal and hippocampal origin. Our results obtained with fiber dissection and conventional histology unambiguously confirmed the connection between the postcommissural fornix and the SMTh, however, due to the nature of these techniques, we could not determine the origin and termination of these fibers. It is possible that they reach the habenula or they only temporarily join the SMTh and terminate in one or more of the thalamic nuclei. Watanabe et al. showed in their study that during brain development, the cells of the nucleus triangularis and the bed nucleus of the anterior commissure belonging to the caudal septal nuclear group originate from the anterior part of the diencephalon (eminentia thalamica) in rats. These cells develop directly behind the foramen of Monro and migrate through the fornix in a rostrodorsal direction to their final location in the septum, while their axons contact the medial habenula via the SMTh. [88, 89] This may explain why some septal fibers follow this route. Weidacker et al. investigated the activity of the human habenula in loss avoidance using functional MRI and described its functional relationship with the hippocampus. [90] Goutagny et al. showed in his electrophysiological study of rats that although we do not know a direct connection between these two structures, there is a functional connection between the lateral habenula and the hippocampus. Moreover, the lateral habenula influences hippocampal theta oscillations and plays a role in memory functions. [91] Aizawa et al. obtained similar results and they described the diagonal band of Broca as a relay station connecting these two areas. [92] The fiber bundle presented in this thesis can represent this connection either directly or through the septal region. However, its exact function and possible clinical significance needs to be clarified in the future.

Our knowledge about the physiological and pathological functioning of the septum is still very incomplete and we can only infer it mainly based on animal experiments. Its role in the reward system was quite early revealed. [93, 94] Currently, most of the information we have is related to the medial septum, which along with the diagonal band of Broca and the nucleus basalis of Meynert forms the most important cholinergic center of the brain. [7] Dysfunction of these areas for any reason, which may be damage or insufficient circulation of the anterior communicating artery or due to neurodegenerative

processes, leads to memory disorders (basal forebrain impairment). [31] One of the most significant relationships of the septal region is the bidirectional septo-hippocampal connection, which is carried out primarily via the precommissural fornix. Through this pathway, the medial septum is not only involved in the cholinergic neuromodulation of the hippocampus, but also plays an important role in the rhythm generation and synchronization of hippocampal theta oscillations, which are also essential for the formation of memory traces. [31] In addition to its memory functions, the theta rhythm generation of the medial septum-diagonal band complex also plays an important role in the motivation of movement (locomotion) initiation. [95] We have much less knowledge about the function of the lateral septum. According to a recent review of Patel, it is primarily involved in processes related to anxiety and it mediates both anxiogenic and anxiolytic effects. [96] The role of the septum also arises in a number of other pathologies and conditions. Using MRI, Butler et al. found enlarged volume of the septal area in patients with temporal lobe epilepsy without mesial temporal sclerosis [97, 98] before the clinical manifestation of Alzheimer’s disease [99] as well as in healthy volunteers with increased accuracy of the source memory. [100] The volume enlargement of this area was also observed in post-mortem dissections in kuru disease. [101] Brisch et al. found a reduced neuronal density of the lateral septum, but without accompanying volume changes in schizophrenic patients. [102]

In addition to its pathological changes, the clinical relevance of the knowledge of the septal region and its connections is given by their use as a potential DBS target. The septum is one of the experimentally earliest stimulated brain areas. Olds and Milner's self-stimulation experiment of rats highlighted the role of the septum in the reward system [93] which was later proven in human subjects as well. [94] However, it has now become clear that the septum has a role in much more complex functions, thus it may be a potential DBS target in several pathologies, primarily those related to the disturbance of hippocampal theta oscillations. [32] Jeong et al. demonstrated in a rat dementia model (basal forebrain cholinergic lesion) that hippocampal cholinergic activity and neurogenesis increased as a result of DBS of the medial septum, and the rats' performance became as good as that of the control animals. [103] The medial septum may therefore be a promising target in Alzheimer's disease or Parkinson's / Lewy body dementia [31] as well as in the case of cognitive dysfunction resulting from traumatic brain injury. [104,

105] Based on animal experiments, stimulation of this area may also be effective in therapy-resistant temporal lobe epilepsy. [33, 106] Although the modern definition of the septum handles it as a separate entity, it should be mentioned that the BNST is also an emerging target region of DBS in the treatment of various psychiatric diseases, primarily in OCD [107] but it may also be effective in major depression [108], anorexia nervosa [109, 110] and addiction. [111, 112] The subgenual cingulate cortex is also an intensively studied region as a DBS target mainly in major depressive disorder. The results of Howell et al. suggest that during stimulation of this area, the cingulum and the forceps minor are the most important connections that are activated and may be responsible for the therapeutic effect. [113] The fiber dissections showed that a bundle of the cingulum originated in the septal nuclei along with the fasciculus inferior of the septum pellucidum, the fibers of which joined the corpus callosum and may reach the PFC through the forceps minor. Therefore, it is possible that DBS of the subgenual area also affects fibers that belong to the septum verum.

DOI:10.14753/SE.2025.3062

6. Conclusions

This thesis aimed to provide a topographical characterization of the subthalamic area with particular interest in the course of the human MFB using fiber dissection, histology and tractography. The MFB could not be identified as a discrete bundle. It is likely that most of the monoaminergic fibers representing the rodent MFB join the ansa lenticularis in the human brain. The existence of the slMFB described using tractography could not be confirmed. [11, 12] These streamlines likely arise from the limitations of the dMRI fiber tracking method. The existence of the limbic cone region of the STN could be verified with fiber connections originating from this region and coursing in the lateral hypothalamus to the GPe and through the ALIC towards the PFC. Moreover, the GPe was identified as a relay station between the limbic cone region of the STN and the PFC.

The topographical anatomy of the human septum verum and its white matter connections was also depicted using fiber dissection supplemented with histological validation. The anatomical knowledge provided by this description is intended to facilitate the safety and accuracy of future DBS therapies, which are currently used only in form of animal experiments.

DOI:10.14753/SE.2025.3062

7. Summary

In this thesis, two brain areas important for DBS were presented using fiber dissection and histological validation.

DBS makes it possible to modulate a specific function of certain brain areas in a reversible way. Accurate anatomical knowledge of the target area is obviously essential for the correct implantation of the stimulation electrodes. The STN is currently the most commonly used target structure primarily stimulated in Parkinson's disease. However, it is surrounded by numerous fiber bundles, the co-stimulation of which may play a role in the triggering of therapeutic or side effects.

One of these fiber bundles – based on tractography studies – is the MFB, which was considered to be responsible for the development of hypomanic side effects. Although this fiber bundle has been extensively studied in rodents, we still only have speculations about its course in the human brain. Based on the results presented in this thesis, most of the monoaminergic fibers representing the MFB join the ansa lenticularis, which was originally described as a pallidothalamic fiber connection, however this latter fact could not be confirmed by fiber dissection. The MFB described by tractography turned out to be a false positive fiber bundle resulting from the limitations of tractography, and is actually made up of the ansa lenticularis, the lenticular fasciculus and the ALIC.

However, stimulation of the slMFB has been emerged as a promising DBS target in the last decade, which - based on the presented results - actually corresponds to the stimulation of the ansa lenticularis in the prerubral region. The therapeutic effect arises most likely due to the activation of the monoaminergic fibers joining it, along with the co-stimulation of the limbic cone region of the medial STN.

While the subthalamic region has been a stimulation target for a relatively long time, the septal region is currently only stimulated in form of animal experiments, but with rather encouraging results. Therefore, it can be expected that in the future the stimulation of this region will also be approved by the authorities as a therapeutic option in human diseases and conditions, for which the topographical anatomical knowledge presented in this thesis will certainly be useful.

8. References

1. Krauss JK, Lipsman N, Aziz T, Boutet A, Brown P, Chang JW, Davidson B, Grill WM, Hariz MI, Horn A, Schulder M, Mammis A, Tass PA, Volkmann J, Lozano AM. Technology of deep brain stimulation: current status and future directions. Nat Rev Neurol. 2021 Feb;17(2):75–87.

2. Lee DJ, Lozano CS, Dallapiazza RF, Lozano AM. Current and future directions of deep brain stimulation for neurological and psychiatric disorders. J Neurosurg. 2019 Aug 1;131(2):333–42.

3. Lozano AM, Lipsman N, Bergman H, Brown P, Chabardes S, Chang JW, Matthews K, McIntyre CC, Schlaepfer TE, Schulder M, Temel Y, Volkmann J, Krauss JK. Deep brain stimulation: current challenges and future directions. Nat Rev Neurol. 2019 Mar;15(3):148–60.

4. Forel A. Untersuchungen über die Haubenregion und ihre oberen Verknüpfungen im Gehirne des Menschen und einiger Säugethiere, mit Beiträgen zu den Methoden der Gehirnuntersuchung. Arch Psychiatr Nervenkr. 1877 Oct;7(3):393–495.

5. Dejerine, J., Dejerine-Klumpke A. Anatomie des Centres Nerveux. Vol. 1. Rueff Paris; 1895. 634–644 p.

6. Parent A, Carpenter MB. Carpenter's human neuroanatomy. Williams & Wilkins; 1996. 716–720; 828–845 p.

7. Nieuwenhuys R, Voogd J, Van Huijzen C. The human central nervous system: a synopsis and atlas. Springer Science & Business Media; 2007. 209–211; 280–286; 291–293; 919–928 p.

8. Baumgartner AJ, Thompson JA, Kern DS, Ojemann SG. Novel targets in deep brain stimulation for movement disorders. Neurosurg Rev. 2022 Aug 5;45(4):2593–613.

9. Mahoney JJ, Koch-Gallup N, Scarisbrick DM, Berry JH, Rezai AR. Deep brain stimulation for psychiatric disorders and behavioral/cognitive-related indications: Review of the literature and implications for treatment. J Neurol Sci. 2022 Jun;437:120253.

10. Mosley PE, Marsh R. The psychiatric and neuropsychiatric symptoms after subthalamic stimulation for Parkinson's disease. J Neuropsychiatry Clin Neurosci. 2015;27(1):19–26.

11. Coenen VA, Honey CR, Hurwitz T, Rahman AA, McMaster J, Bürgel U, Mädler B. Medial forebrain bundle stimulation as a pathophysiological mechanism for hypomania in subthalamic nucleus deep brain stimulation for Parkinson's disease. Neurosurgery. 2009 Jun;64(6):1106–15.

12. Coenen VA, Panksepp J, Hurwitz TA, Urbach H, Mädler B. Human Medial Forebrain Bundle (MFB) and Anterior Thalamic Radiation (ATR): Imaging of Two Major Subcortical Pathways and the Dynamic Balance of Opposite Affects in Understanding Depression. J Neuropsychiatry Clin Neurosci. 2012 Jan;24(2):223–36.

13. Schlaepfer TE, Bewernick BH, Kayser S, Mädler B, Coenen VA. Rapid Effects of Deep Brain Stimulation for Treatment-Resistant Major Depression. Biol Psychiatry. 2013 Jun;73(12):1204–12.

14. Bracht T, Doidge AN, Keedwell PA, Jones DK. Hedonic tone is associated with left supero-lateral medial forebrain bundle microstructure. Psychol Med. 2015 Mar;45(4):865–74.

15. Bracht T, Horn H, Strik W, Federspiel A, Schnell S, Höfle O, Stegmayer K, Wiest R, Dierks T, Müller TJ, Walther S. White matter microstructure alterations of the medial forebrain bundle in melancholic depression. J Affect Disord. 2014 Feb;155:186–93.

16. Bracht T, Linden D, Keedwell P. A review of white matter microstructure alterations of pathways of the reward circuit in depression. J Affect Disord. 2015 Nov 15;187:45–53.

17. Bracht T, Jones DK, Müller TJ, Wiest R, Walther S. Limbic white matter microstructure plasticity reflects recovery from depression. J Affect Disord. 2015 Jan 1;170:143–9.

18. Anthofer JM, Steib K, Fellner C, Lange M, Brawanski A, Schlaier J. DTI-based

deterministic fibre tracking of the medial forebrain bundle. Acta Neurochir (Wien). 2015 Mar;157(3):469–77.

19. Hana A, Hana A, Dooms G, Boecher-Schwarz H, Hertel F. Visualization of the medial forebrain bundle using diffusion tensor imaging. Front Neuroanat. 2015;9:139.

20. Owens JA, Spitz G, Ponsford JL, Dymowski AR, Ferris N, Willmott C. White matter integrity of the medial forebrain bundle and attention and working memory deficits following traumatic brain injury. Brain Behav. 2017 Feb;7(2):e00608.

21. Hosp JA, Coenen VA, Rijntjes M, Egger K, Urbach H, Weiller C, Reisert M. Ventral tegmental area connections to motor and sensory cortical fields in humans. Brain Struct Funct. 2019 Nov;224(8):2839–55.

22. Coenen VA, Döbrössy MD, Teo SJ, Wessolleck J, Sajonz BEA, Reinacher PC, Thierauf-Emberger A, Spittau B, Leupold J, von Elverfeldt D, Schlaepfer TE, Reisert M. Diverging prefrontal cortex fiber connection routes to the subthalamic nucleus and the mesencephalic ventral tegmentum investigated with long range (normative) and short range (ex-vivo high resolution) 7T DTI. Brain Struct Funct. 2022 Jan;227(1):23–47.

23. Fenoy AJ, Schulz P, Selvaraj S, Burrows C, Spiker D, Cao B, Zunta-Soares G, Gajwani P, Quevedo J, Soares J. Deep brain stimulation of the medial forebrain bundle: Distinctive responses in resistant depression. J Affect Disord. 2016 Oct;203:143–51.

24. Fenoy AJ, Schulz PE, Selvaraj S, Burrows CL, Zunta-Soares G, Durkin K, Zanotti-Fregonara P, Quevedo J, Soares JC. A longitudinal study on deep brain stimulation of the medial forebrain bundle for treatment-resistant depression. Transl Psychiatry. 2018 Jun 4;8(1):111.

25. Coenen VA, Bewernick BH, Kayser S, Kilian H, Boström J, Greschus S, Hurlemann R, Klein ME, Spanier S, Sajonz B, Urbach H, Schlaepfer TE. Superolateral medial forebrain bundle deep brain stimulation in major depression: a gateway trial. Neuropsychopharmacology. 2019 Jun 13;44(7):1224–32.

26. Coenen VA, Schlaepfer TE, Goll P, Reinacher PC, Voderholzer U, Tebartz van Elst L, Urbach H, Freyer T. The medial forebrain bundle as a target for deep brain stimulation for obsessive-compulsive disorder. CNS Spectr. 2017 Jun 8;22(3):282–9.

27. Andy OJ, Stephan H. The septum in the human brain. J Comp Neurol. 1968 Jul;133(3):383–410.

28. Horváth S, Palkovits M. Morphology of the human septal area: a topographic atlas. Acta Morphol Hung. 1987;35(3–4):157–74.

29. Jacques S. Brain stimulation and reward: “pleasure centers” after twenty-five years. Neurosurgery. 1979 Aug;5(2):277–83.

30. Baumeister AA. The Tulane Electrical Brain Stimulation Program a historical case study in medical ethics. J Hist Neurosci. 2000 Dec;9(3):262–78.

31. Tsanov M. Basal forebrain impairment: Understanding the mnemonic function of the septal region translates in therapeutic advances. Front Neural Circuits. 2022;16:916499.

32. Takeuchi Y, Nagy AJ, Barcsai L, Li Q, Ohsawa M, Mizuseki K, Berényi A. The medial septum as a potential target for treating brain disorders associated with oscillopathies. Front Neural Circuits. 2021;15:701080.

33. Cole ER, Grogan DP, Laxpati NG, Fernandez AM, Skelton HM, Isbaine F, Gutekunst CA, Gross RE. Evidence supporting deep brain stimulation of the medial septum in the treatment of temporal lobe epilepsy. Epilepsia. 2022 Sep;63(9):2192–213.

34. Kundu B, Brock AA, Englot DJ, Butson CR, Rolston JD. Deep brain stimulation for the treatment of disorders of consciousness and cognition in traumatic brain injury patients: a review. Neurosurg Focus. 2018 Aug;45(2):E14.

35. ConnectomeDB, Human Connectome Project [Internet]. [Last updated: April, 2018]. Available from: https://db.humanconnectome.org/

36. Klingler J. Erleichterung der makroskopischen Präparation des Gehirns durch den

Gefrierprozess. Schweiz Arch Neurol und Psychiatr. 1935;(36):247–256.

37. Krutsay M. Silver impregnation of neurofibrils in paraffin sections . Anat Anz. 1987;164(1):77–80.

38. Tournier JD, Smith R, Raffelt D, Tabbara R, Dhollander T, Pietsch M, Christiaens D, Jeurissen B, Yeh CH, Connelly A. MRtrix3: A fast, flexible and open software framework for medical image processing and visualisation. Neuroimage. 2019 Nov;202:116137.

39. Tournier JD, Calamante F, Connelly A. Improved probabilistic streamlines tractography by 2nd order integration over fibre orientation distributions. Proc Intl Soc Mag Reson Med. 2010;18.

40. Jeurissen B, Tournier JD, Dhollander T, Connelly A, Sijbers J. Multi-tissue constrained spherical deconvolution for improved analysis of multi-shell diffusion MRI data. Neuroimage. 2014 Dec;103:411–26.

41. Dhollander T, Mito R, Raffelt D, Connelly A. Improved white matter response function estimation for 3-tissue constrained spherical deconvolution. In: Proc Intl Soc Mag Reson Med. 2019.

42. Meszaros C, Kurucz P, Baksa G, Alpar A, Ganslandt O, Brandner S, Barany L. Topographical anatomy of the subthalamic region with special interest in the human medial forebrain bundle. J Neurosurg. 2024 Mar 15;1–11.

43. Trutti AC, Mulder MJ, Hommel B, Forstmann BU. Functional neuroanatomical review of the ventral tegmental area. Neuroimage. 2019 May;191:258–68.

44. Baron MS, Sidibé M, DeLong MR, Smith Y. Course of motor and associative pallidothalamic projections in monkeys. J Comp Neurol. 2001 Jan 15;429(3):490–501.

45. Lavoie B, Smith Y, Parent A. Dopaminergic innervation of the basal ganglia in the squirrel monkey as revealed by tyrosine hydroxylase immunohistochemistry. J Comp Neurol. 1989 Nov 1;289(1):36–52.

46. Cossette M, Lévesque M, Parent A. Extrastriatal dopaminergic innervation of

human basal ganglia. Neurosci Res. 1999 May;34(1):51–4.

47. Prensa L, Cossette M, Parent A. Dopaminergic innervation of human basal ganglia. J Chem Neuroanat. 2000 Dec;20(3–4):207–13.

48. Parent M, Wallman MJ, Gagnon D, Parent A. Serotonin innervation of basal ganglia in monkeys and humans. J Chem Neuroanat. 2011 Jul;41(4):256–65.

49. Haynes WIA, Haber SN. The Organization of Prefrontal-Subthalamic Inputs in Primates Provides an Anatomical Substrate for Both Functional Specificity and Integration: Implications for Basal Ganglia Models and Deep Brain Stimulation. J Neurosci. 2013 Mar 13;33(11):4804–14.

50. Haber SN, Yendiki A, Jbabdi S. Four Deep Brain Stimulation Targets for Obsessive-Compulsive Disorder: Are They Different? Biol Psychiatry. 2021 Nov;90(10):667–77.

51. Haber SN, Liu H, Seidlitz J, Bullmore E. Prefrontal connectomics: from anatomy to human imaging. Neuropsychopharmacology. 2022 Jan;47(1):20–40.

52. Coenen VA, Schlaepfer TE, Sajonz B, Döbrössy M, Kaller CP, Urbach H, Reisert M. Tractographic description of major subcortical projection pathways passing the anterior limb of the internal capsule. Corticopetal organization of networks relevant for psychiatric disorders. NeuroImage Clin. 2020;25:102165.

53. Rheault F, Poulin P, Valcourt Caron A, St-Onge E, Descoteaux M. Common misconceptions, hidden biases and modern challenges of dMRI tractography. J Neural Eng. 2020 Feb 18;17(1):011001.

54. Fenoy AJ, Quevedo J, Soares JC. Deep brain stimulation of the “medial forebrain bundle”: a strategy to modulate the reward system and manage treatment-resistant depression. Mol Psychiatry. 2022 Jan 26;27(1):574–92.

55. Coenen VA, Watakabe A, Skibbe H, Yamamori T, Döbrössy MD, Sajonz BEA, Reinacher PC, Reisert M. Tomographic tract tracing and data driven approaches to unravel complex 3D fiber anatomy of DBS relevant prefrontal projections to the diencephalic-mesencephalic junction in the marmoset. Brain Stimul. 2023 Apr 6;16(2):670–81.

56. Barbier M, Risold PY. Understanding the Significance of the Hypothalamic Nature of the Subthalamic Nucleus. eneuro. 2021 Sep;8(5):ENEURO.0116-21.2021.

57. Saga Y, Hoshi E, Tremblay L. Roles of Multiple Globus Pallidus Territories of Monkeys and Humans in Motivation, Cognition and Action: An Anatomical, Physiological and Pathophysiological Review. Front Neuroanat. 2017 Apr 10;11.

58. Saad P, Shendrik KS, Karroum PJ, Azizi H, Jolayemi A. The Anterior Globus Pallidus Externus of Basal Ganglia as Primarily a Limbic and Associative Territory. Cureus. 2020 Dec 2;

59. Adler A, Joshua M, Finkes I, Bergman H. High-Frequency Stimulation of the Globus Pallidus External Segment Biases Behavior Toward Reward. In: The Basal Ganglia IX. Springer; 2009. p. 85–96.

60. Baumann B, Danos P, Krell D, Diekmann S, Leschinger A, Stauch R, Wurthmann C, Bernstein HG, Bogerts B. Reduced Volume of Limbic System–Affiliated Basal Ganglia in Mood Disorders: J Neuropsychiatry Clin Neurosci. 1999 Feb;11(1):71–8.

61. Barany L, Meszaros C, Ganslandt O, Buchfelder M, Kurucz P. Neural and vascular architecture of the septum pellucidum: an anatomical study and considerations for safe endoscopic septum pellucidotomy. J Neurosurg. 2019 Aug 2;133(3):902–11.

62. Kochanski RB, Dawe R, Eddelman DB, Kocak M, Sani S. Identification of the stria medullaris thalami using diffusion tensor imaging. NeuroImage Clin. 2016;12:852–7.

63. Roddy DW, Roman E, Rooney S, Andrews S, Farrell C, Doolin K, Levins KJ, Tozzi L, Tierney P, Barry D, Frodl T, O'Keane V, O'Hanlon E. Awakening neuropsychiatric research into the stria medullaris: Development of a diffusion-weighted imaging tractography protocol of this key limbic structure. Front Neuroanat. 2018;12:39.

64. Kwon HG, Byun WM, Ahn SH, Son SM, Jang SH. The anatomical characteristics of the stria terminalis in the human brain: a diffusion tensor tractography study. Neurosci Lett. 2011 Aug 15;500(2):99–102.

65. Kamali A, Yousem DM, Lin DD, Sair HI, Jasti SP, Keser Z, Riascos RF, Hasan KM. Mapping the trajectory of the stria terminalis of the human limbic system using high spatial resolution diffusion tensor tractography. Neurosci Lett. 2015 Nov 3;608:45–50.

66. Li M, Zhang Z, Wu X, Wang X, Liu X, Liang J, Chen G, Feng Y, Li M. Tractography of the stria terminalis in the human brain. Clin Anat. 2022 Apr;35(3):383–91.

67. Klingler J, Gloor P. The connections of the amygdala and of the anterior temporal cortex in the human brain. J Comp Neurol. 1960 Dec;115:333–69.

68. Cho ZH, Law M, Chi JG, Choi SH, Park SY, Kammen A, Park CW, Oh SH, Kim YB. An anatomic review of thalamolimbic fiber tractography: ultra-high resolution direct visualization of thalamolimbic fibers anterior thalamic radiation, superolateral and inferomedial medial forebrain bundles, and newly identified septum pellucidum tract. World Neurosurg. 2015 Jan;83(1):54-61.e32.

69. Cho ZH, Chi JG, Choi SH, Oh SH, Park SY, Paek SH, Park CW, Calamante F, Kim YB. A newly identified frontal path from fornix in septum pellucidum with 7.0T MRI track density imaging (TDI) - The septum pellucidum tract (SPT). Front Neuroanat. 2015;9:151.

70. Ferner, H. R., & Pernkopf E. Atlas der topographischen und angewandten Anatomie des Menschen. Urban & Schwarzenberg; 1963. 772 p.

71. Gudden B. Beitrag zur Kenntniss des Corpus mammillare und der sogenannten Schenkel des Fornix. Arch Psychiatr Nervenkr. 1881;11(2):428–52.

72. Honegger J. Vergleichend-anatomische Untersuchungen über den Fornix und die zu ihm in Beziehung gebrachten Gebilde im Gehirn des Menschen und der Säugethiere. Buchdruckerei Aubert-Schuchardt. 1890;5.

73. Lotheissen G. Uber die Stria Medullaris Thalami Optici und Ihre Verbindungen: Vergleichend-Anatomische Studie. Anat Hefte. 1894;4(2):225–59.

74. Kölliker A. Ueber den Fornix longus von Forel und die Riechstrahlungen im Gehirn des Kaninchens. 1894;

75. Edinger, L., & Wallenberg A. Untersuchungen über den Fornix und das Corpus mamillare. Arch Psychiatr Nervenkr. 1901;35(1):1–21.

76. y Cajal SR. Histologie du système nerveux de l'homme & des vertébrés: Cervelet, cerveau moyen, rétine, couche optique, corps strié, écorce cérébrale générale & régionale, grand sympathique. A Maloine. 1911;2.

77. Humphrey T. The telencephalon of the bat. I. The non-cortical nuclear masses and certain pertinent fiber connections. 1936;

78. Young MW. The nuclear pattern and fiber connections of the non-cortical centers of the telencephalon of the rabbit (Lepus cuniculus). 1936;

79. Marburg O. The structure and fiber connections of the human habenula. J Comp Neurol. 1944;80(2):211–33.

80. Sprague JM, Meyer M. An experimental study of the fornix in the rabbit. J Anat. 1950 Oct;84(4):354–68.

81. Nauta WJ. An experimental study of the fornix system in the rat. J Comp Neurol. 1956 Apr;104(2):247–71.

82. Raisman G. The connexions of the septum. Brain. 1966 Jun;89(2):317–48.

83. Guillery RW. Degeneration in the post-commissural fornix and the mamillary peduncle of the rat. J Anat. 1956 Jul;90(3):350–70.

84. Powell TP, Cowan WM. An experimental study of the efferent connexions of the hippocampus. Brain. 1955;78(1):115–32.

85. Powell TP, Guillery RW, Cowan WM. A quantitative study of the fornixmamillo-thalamic system. J Anat. 1957 Oct;91(4):419–37.

86. Valenstein ES, Nauta WJ. A comparison of the distribution of the fornix system in the rat, guinea pig, cat, and monkey. J Comp Neurol. 1959 Dec;113:337–63.

87. Votaw CL, Lauer EW. An afferent hippocampal fiber system in the fornix of the monkey. J Comp Neurol. 1963 Oct;121:195–206.

88. Watanabe K, Irie K, Hanashima C, Takebayashi H, Sato N. Diencephalic

progenitors contribute to the posterior septum through rostral migration along the hippocampal axonal pathway. Sci Rep. 2018 Aug 6;8(1):11728.

89. Watanabe K, Takebayashi H, Sato N. The fornix acts as a permissive corridor for septal neuron migration beyond the diencephalic-telencephalic boundary. Sci Rep. 2020 May 20;10(1):8315.

90. Weidacker K, Kim SG, Nord CL, Rua C, Rodgers CT, Voon V. Avoiding monetary loss: A human habenula functional MRI ultra-high field study. Cortex. 2021 Sep;142:62–73.

91. Goutagny R, Loureiro M, Jackson J, Chaumont J, Williams S, Isope P, Kelche C, Cassel JC, Lecourtier L. Interactions between the lateral habenula and the hippocampus: implication for spatial memory processes. Neuropsychopharmacology. 2013 Nov;38(12):2418–26.

92. Aizawa H, Yanagihara S, Kobayashi M, Niisato K, Takekawa T, Harukuni R, McHugh TJ, Fukai T, Isomura Y, Okamoto H. The synchronous activity of lateral habenular neurons is essential for regulating hippocampal theta oscillation. J Neurosci. 2013 May 15;33(20):8909–21.

93. Olds J, Milner P. Positive reinforcement produced by electrical stimulation of septal area and other regions of rat brain. J Comp Physiol Psychol. 1954 Dec;47(6):419–27.

94. Heath RG. Electrical self-stimulation of the brain in man. Am J Psychiatry. 1963 Dec;120:571–7.

95. Mocellin P, Mikulovic S. The role of the medial septum-associated networks in controlling locomotion and motivation to move. Front Neural Circuits. 2021;15:699798.

96. Patel H. The role of the lateral septum in neuropsychiatric disease. J Neurosci Res. 2022 Jul;100(7):1422–37.

97. Butler T, Zaborszky L, Wang X, McDonald CR, Blackmon K, Quinn BT, DuBois J, Carlson C, Barr WB, French J, Kuzniecky R, Halgren E, Devinsky O, Thesen T. Septal nuclei enlargement in human temporal lobe epilepsy without mesial

temporal sclerosis. Neurology. 2013 Jan 29;80(5):487–91.

98. Butler T, Zaborszky L, Pirraglia E, Li J, Wang XH, Li Y, Tsui W, Talos D, Devinsky O, Kuchna I, Nowicki K, French J, Kuzniecky R, Wegiel J, Glodzik L, Rusinek H, DeLeon MJ, Thesen T. Comparison of human septal nuclei MRI measurements using automated segmentation and a new manual protocol based on histology. Neuroimage. 2014 Aug 15;97:245–51.

99. Butler T, Harvey P, Deshpande A, Tanzi E, Li Y, Tsui W, Silver C, Fischer E, Wang X, Chen J, Rusinek H, Pirraglia E, Osorio RS, Glodzik L, de Leon MJ. Basal forebrain septal nuclei are enlarged in healthy subjects prior to the development of Alzheimer's disease. Neurobiol Aging. 2018 May;65:201–5.

100. Butler T, Blackmon K, Zaborszky L, Wang X, DuBois J, Carlson C, Barr WB, French J, Devinsky O, Kuzniecky R, Halgren E, Thesen T. Volume of the human septal forebrain region is a predictor of source memory accuracy. J Int Neuropsychol Soc. 2012 Jan;18(1):157–61.

101. Beck E, Daniel PM, Alpers M, Gajdusek DC, Gibbs CJ. Experimental "kuru" in chimpanzees. A pathological report. Lancet (London, England). 1966 Nov 12;2(7472):1056–9.

102. Brisch R, Bernstein HG, Dobrowolny H, Krzyżanowska M, Jankowski Z, Bogerts B, Gos T. Volumetric analysis of the diagonal band of Broca in patients with schizophrenia and affective disorders: A post-mortem study. Clin Anat. 2016 May;29(4):466–72.

103. Jeong DU, Lee JE, Lee SE, Chang WS, Kim SJ, Chang JW. Improvements in memory after medial septum stimulation are associated with changes in hippocampal cholinergic activity and neurogenesis. Biomed Res Int. 2014;2014:568587.

104. Lee DJ, Gurkoff GG, Izadi A, Berman RF, Ekstrom AD, Muizelaar JP, Lyeth BG, Shahlaie K. Medial septal nucleus theta frequency deep brain stimulation improves spatial working memory after traumatic brain injury. J Neurotrauma. 2013 Jan 15;30(2):131–9.

105. Lee DJ, Gurkoff GG, Izadi A, Seidl SE, Echeverri A, Melnik M, Berman RF, Ekstrom AD, Muizelaar JP, Lyeth BG, Shahlaie K. Septohippocampal Neuromodulation Improves Cognition after Traumatic Brain Injury. J Neurotrauma. 2015 Nov 15;32(22):1822–32.

106. Fisher RS. Stimulation of the medial septum should benefit patients with temporal lobe epilepsy. Med Hypotheses. 2015 Jun;84(6):543–50.

107. Luyten L, Hendrickx S, Raymaekers S, Gabriëls L, Nuttin B. Electrical stimulation in the bed nucleus of the stria terminalis alleviates severe obsessive-compulsive disorder. Mol Psychiatry. 2016 Sep;21(9):1272–80.

108. Fitzgerald PB, Segrave R, Richardson KE, Knox LA, Herring S, Daskalakis ZJ, Bittar RG. A pilot study of bed nucleus of the stria terminalis deep brain stimulation in treatment-resistant depression. Brain Stimul. 2018;11(4):921–8.

109. Blomstedt P, Naesström M, Bodlund O. Deep brain stimulation in the bed nucleus of the stria terminalis and medial forebrain bundle in a patient with major depressive disorder and anorexia nervosa. Clin case reports. 2017 May;5(5):679–84.

110. Manuelli M, Franzini A, Galentino R, Bidone R, Dell'Osso B, Porta M, Servello D, Cena H. Changes in eating behavior after deep brain stimulation for anorexia nervosa. A case study. Eat Weight Disord. 2020 Oct;25(5):1481–6.

111. Gonçalves-Ferreira A, do Couto FS, Rainha Campos A, Lucas Neto LP, Gonçalves-Ferreira D, Teixeira J. Deep Brain Stimulation for Refractory Cocaine Dependence. Biol Psychiatry. 2016 Jun 1;79(11):e87-9.

112. Heldmann M, Berding G, Voges J, Bogerts B, Galazky I, Müller U, Baillot G, Heinze HJ, Münte TF. Deep brain stimulation of nucleus accumbens region in alcoholism affects reward processing. PLoS One. 2012;7(5):e36572.

113. Howell B, Choi KS, Gunalan K, Rajendra J, Mayberg HS, McIntyre CC. Quantifying the axonal pathways directly stimulated in therapeutic subcallosal cingulate deep brain stimulation. Hum Brain Mapp. 2019 Feb 15;40(3):889–903.

DOI:10.14753/SE.2025.3062

9. Bibliography of the candidate's publications

9.1. Publication related to this thesis

Meszaros C, Kurucz P, Baksa G, Alpar A, Ganslandt O, Brandner S, Barany L. Topographical anatomy of the subthalamic region with special interest in the human medial forebrain bundle. J Neurosurg. Published online March 15, 2024:1-11. (IF: 4,1)

9.2. Publications independent of this thesis

Barany L, **Meszaros C**, Ganslandt O, Buchfelder M, Kurucz P. Neural and vascular architecture of the septum pellucidum: an anatomical study and considerations for safe endoscopic septum pellucidotomy. J Neurosurg. 2020;133(3). (IF: 5,115)

Kurucz P, **Meszaros C**, Ganslandt O, Buchfelder M, Barany L. The "Valva Cerebri": Morphometry, Topographic Anatomy and Histology of the Rhomboid Membrane at the Craniocervical Junction. Clin Anat. 2020;33(1). (IF: 2,414)

DOI:10.14753/SE.2025.3062

10. Acknowledgements

I would like to express my gratitude to my supervisors, **Dr. László Bárány**, from whom I learned all the preparation techniques and got loads of support during the whole time working on this thesis, and **Prof. Dr. Alán Alpár** for his professional support.

Also, to **Dr. Gábor Baksa** for his technical and professional support during the preparation and histological procedures, to **Dr. Péter Kurucz** and **Prof. Dr. Oliver Ganslandt** for their professional advices.

I am also grateful to **Mária Bakó**, from whom I had the good fortune to learn the basics of histological processing as well as to **Péterné Horváth** for her support during the histological preparations. I also would like to thank to **Ferenc Szabó** for his help during the preparation of the cadavers.

Furthermore, I would like to thank to my family for their support during and after my studies and research.

Last but not least, I would like to express my respect to all those who donated their bodies to the Department of Anatomy, Histology and Embryology of the Semmelweis University, thereby making this thesis possible.